Check for updates

Geochemistry, Geophysics, Geosystems®

AGU ADVANCING EARTH AND SPACE SCIENCES

RESEARCH ARTICLE
10.1029/2023GC011302

Impact of Seawater Inorganic Carbon Chemistry on Element Incorporation in Foraminiferal Shell Carbonate

S. Karancz[1], L. J. de Nooijer[1], G. J. A. Brummer[1], J. Lattaud[2], N. Haghipour[2,3], Y. Rosenthal[4], and G. J. Reichart[1,5]

[1]NIOZ-Royal Netherlands Institute for Sea Research, Texel, The Netherlands, [2]Department of Earth Sciences, Biogeoscience Group, ETH Zürich, Zürich, Switzerland, [3]Laboratory of Ion Beam Physics, ETH Zürich, Zürich, Switzerland, [4]Department of Marine and Coastal Sciences, Rutgers University, State University of New Jersey, New Brunswick, NJ, USA, [5]Department of Earth Sciences, Utrecht University, Utrecht, The Netherlands

Key Points:

- S/Ca in the planktonic foraminifera, *Globigerina bulloides*, *Globigerinoides ruber*, *Trilobatus sacculifer*, and *Neogloboquadrina incompta* show a positive correlation with [CO_3^{2-}]
- Seawater [HCO_3^-] may have a stronger influence on the incorporation of magnesium in the foraminifera's shells than salinity
- A multi-element approach may correct for the influence of multiple controls on the incorporation of elements

Supporting Information:

Supporting Information may be found in the online version of this article.

Correspondence to:

S. Karancz,
szabina.karancz@nioz.nl

Citation:

Karancz, S., de Nooijer, L. J., Brummer, G. J. A., Lattaud, J., Haghipour, N., Rosenthal, Y., & Reichart, G. J. (2024). Impact of seawater inorganic carbon chemistry on element incorporation in foraminiferal shell carbonate. *Geochemistry, Geophysics, Geosystems*, *25*, e2023GC011302. https://doi.org/10.1029/2023GC011302

Received 13 OCT 2023
Accepted 20 FEB 2024

Abstract Reconstruction of the marine inorganic carbon system relies on proxy signal carriers, such as element/calcium (El/Ca) ratios in foraminiferal shells. Concentrations of boron, lithium, strontium, and sulfur have been shown to vary with carbonate system parameters, but when comparing individual proxy reconstructions based on these elements, they are rarely in complete agreement. This is likely caused by the simultaneous effects of multiple environmental factors on element incorporation. Culture experiments with benthic foraminifera have revealed that the shell's S/Ca reflects the carbon chemistry and can potentially be used as a proxy for seawater [CO_3^{2-}]. Aiming to investigate the application potential of sulfur incorporation for carbonate speciation reconstruction, we present S/Ca ratios in five planktonic foraminiferal species, namely *Globigerina bulloides*, *Globigerinoides ruber albus*, *Globigerinoides ruber ruber*, *Trilobatus sacculifer*, and *Neogloboquadrina incompta* from core-top sediments in regions with contrasting [CO_3^{2-}], [HCO_3^-], temperature, and salinity. Analyses of B/Ca and Mg/Ca ratios are included here since these elements have been shown to depend to a certain degree on carbon system parameters (e.g., calcite saturation state and pH, respectively) as well. Moreover, foraminiferal Mg/Ca values covary with S/Ca values and thereby might compromise its proxy application. In contrast to previously published results, this new data set shows a positive correlation between the incorporation of sulfur in the foraminifer's shell and seawater [CO_3^{2-}]. As the incorporation of sulfur and magnesium are positively correlated, S/Mg values of the same foraminifera may be used to improve inorganic carbon system reconstructions.

Plain Language Summary Ions incorporated in the shells of foraminifera, a group of unicellular calcifying organisms, provide crucial insight into past changes in the ocean's carbon chemistry. Inorganic carbon chemistry includes six parameters: [CO_2], [HCO_3^-], [CO_3^{2-}], pH, dissolved inorganic carbon concentration, and total alkalinity; and previous studies have shown that the incorporation of sulfur, magnesium, and boron depend on one or more of these parameters. We analyzed sulfur, magnesium, and boron concentrations in planktonic foraminifera from regions with various carbon chemistry conditions to investigate the application potential of these elements in reconstructing parameters of carbon chemistry. Results of this field study indicate that [HCO_3^-] may also have a strong influence on the incorporation of magnesium in addition to the previously reported temperature, salinity, and pH control, and the sulfur concentrations in foraminifera are likely affected by more than one parameter of the carbon chemistry. A significant positive correlation between sulfur and magnesium concentrations hints at shared parameters controlling their incorporations. Therefore, taking the ratio of sulfur and magnesium concentrations may correct the parameters that influence the incorporation of both elements. Here, we suggest investigating the potential of combining multiple elements in future work for better constraining the marine inorganic carbon chemistry.

1. Introduction

Because of the ocean's large role in mitigating anthropogenic carbon, predicting the effects of future climate change relies on understanding the processes involved, such as the ocean uptake of CO_2 and its reaction with water, and this can be achieved through reconstructions of past atmospheric CO_2 levels and ocean chemistry. The complete marine inorganic carbon chemistry can be computed when at least two of its six parameters (pCO_2, dissolved inorganic carbon concentration ([DIC]), [CO_3^{2-}], [HCO_3^-], pH and total alkalinity) are known (Zeebe & Wolf-Gladrow, 2001). A suite of geochemical proxies has been applied to reconstruct changes in the

© 2024 The Authors. Geochemistry, Geophysics, Geosystems published by Wiley Periodicals LLC on behalf of American Geophysical Union.
This is an open access article under the terms of the Creative Commons Attribution License, which permits use, distribution and reproduction in any medium, provided the original work is properly cited.

15252027, 2024, 4, Downloaded from https://agupubs.onlinelibrary.wiley.com/doi/10.1029/2023GC011302 by Cochrane Netherlands, Wiley Online Library on [19/04/2024]. See the Terms and Conditions (https://onlinelibrary.wiley.com/terms-and-conditions) on Wiley Online Library for rules of use; OA articles are governed by the applicable Creative Commons License

parameters of the ocean's carbonate system, both subrecent (e.g., Hönisch & Hemming, 2005; Raitzsch et al., 2018) and in deep time (e.g., Müller et al., 2020; Pagani et al., 2005). Commonly applied isotopic ratio-based proxies for past sea water carbon reconstructions include the boron isotopic composition of calcareous organisms (e.g., corals, foraminifera; Foster & Rae, 2016; Hemming & Hanson, 1992) and the carbon isotopic composition of alkenones (long-chained unsaturated methyl and ethyl n-ketones; Pagani, 2014; Pagani et al., 2002). Although these proxies provided crucial insights into past variability in pH and pCO_2, respectively, they are limited by some fundamental issues.

One of these fundamental issues is that the application of B-isotopes requires an independent additional carbon system parameter (e.g., alkalinity) and for instance the application of carbon isotopes of alkenones is limited by physiological fractionation. As the reconstruction of the complete marine inorganic carbon system requires an estimate of at least two of its parameters (Zeebe & Wolf-Gladrow, 2001), multiple proxies are often applied simultaneously. As such proxies, a suite of planktic foraminiferal element concentrations were suggested: B/Ca (Allen & Hönisch, 2012; Allen et al., 2012; Haynes et al., 2017; Yu & Elderfield, 2007; Yu et al., 2007) and U/Ca (Raitzsch et al., 2011; Russell et al., 2004) reflecting $[B(OH)_4]/[HCO_3^-]$ and $[CO_3^{2-}]$, respectively. However, there is an ongoing debate about whether the incorporation of these elements into the foraminifer's shell depends on only one parameter of the carbonate system (Babila et al., 2014; Guo et al., 2019). For instance, B/Ca reflects $[B(OH)_4^-]/[HCO_3^-]$ (Allen et al., 2011; Yu et al., 2007), but is also suggested to respond to changes in salinity (Allen et al., 2011, 2012) and $[PO_4^{3-}]$ (Henehan et al., 2015).

Van Dijk, de Nooijer, Wolthers, and Reichart (2017) and Van Dijk, de Nooijer, Boer, and Reichart (2017) recently proposed a novel proxy based on sulfur incorporation in the foraminiferal shell carbonate targeting seawater inorganic carbon chemistry. If S/Ca faithfully records seawater $[CO_3^{2-}]$, it could provide a second constraint on the carbon system and therefore allow for reconstruction of pCO_2. However, this potential novel proxy for seawater $[CO_3^{2-}]$ (i.e., S/Ca; Van Dijk, de Nooijer, Wolthers, & Reichart, 2017; Van Dijk, de Nooijer, Boer, & Reichart, 2017) may be affected by other parameters of the inorganic carbon system, and also, the existing calibration for foraminiferal S/Ca to the carbon system is based on controlled growth experiments.

Results from inorganic calcite growth experiments suggest that carbonate system parameters may not be the only factor affecting sulfur uptake in the $CaCO_3$ (Busenberg & Plummer, 1985; Kitano et al., 1975). These experiments showed that precipitation rate and incorporation of other elements also affect calcite S/Ca values, which is important as such confounding factors potentially complicate the application of El/Ca ratios. For instance, the analysis of the within-shell distribution of sulfur and magnesium in benthic foraminifera revealed a co-variance between these two elements, suggesting that common parameters may affect their incorporations (Van Dijk et al., 2019). The Mg/Ca values in the foraminiferal shell carbonate are a popular tool for reconstructing seawater temperature (Anand et al., 2003; Lea et al., 1999; Rosenthal et al., 1997), but are also known to be affected by multiple other factors. Already when introduced as a temperature proxy, the impact of salinity on Mg/Ca was acknowledged (Lea et al., 1999; Nürnberg et al., 1996). In addition, the carbonate system is known to affect the incorporation of Mg in the foraminifera shell, both from culture and field calibrations (Dueñas-Bohórquez et al., 2009; Evans et al., 2016; Gray & Evans, 2019; Gray et al., 2018; Kısakürek et al., 2008; Lea et al., 1999), thereby potentially offsetting paleotemperature estimates. These inter-related proxy relations resulted in proxy calibrations based on multiple environmental variables being included in calibrations (Rosenthal et al., 2022 and references therein).

Here we present new foraminiferal shell element data from a field survey (from 30 sites) targeting areas with contrasting carbonate chemistry to unravel the impact of different factors on the application of S/Ca, B/Ca, and Mg/Ca in foraminifera as carbonate system proxies. At the same time, the effect of other confounding environmental parameters (e.g., seawater temperature) on element incorporation was assessed. As earlier studies investigated the S/Ca values only in benthic foraminifera that differ both in element incorporations and isotopic fractionation from the planktonic ones (Van Dijk, de Nooijer, Boer, & Reichart, 2017; Van Dijk, de Nooijer, Wolthers, & Reichart, 2017; Van Dijk et al., 2019), this study reports for the first time results from planktonic foraminiferal species. We use these results to explore new element/element ratios as proxies for the different components of the marine inorganic carbon system.

15252027, 2024, 4, Downloaded from https://agupubs.onlinelibrary.wiley.com/doi/10.1029/2023GC011302 by Cochrane Netherlands, Wiley Online Library on [19/04/2024]. See the Terms and Conditions (https://onlinelibrary.wiley.com/terms-and-conditions) on Wiley Online Library for rules of use; OA articles are governed by the applicable Creative Commons License

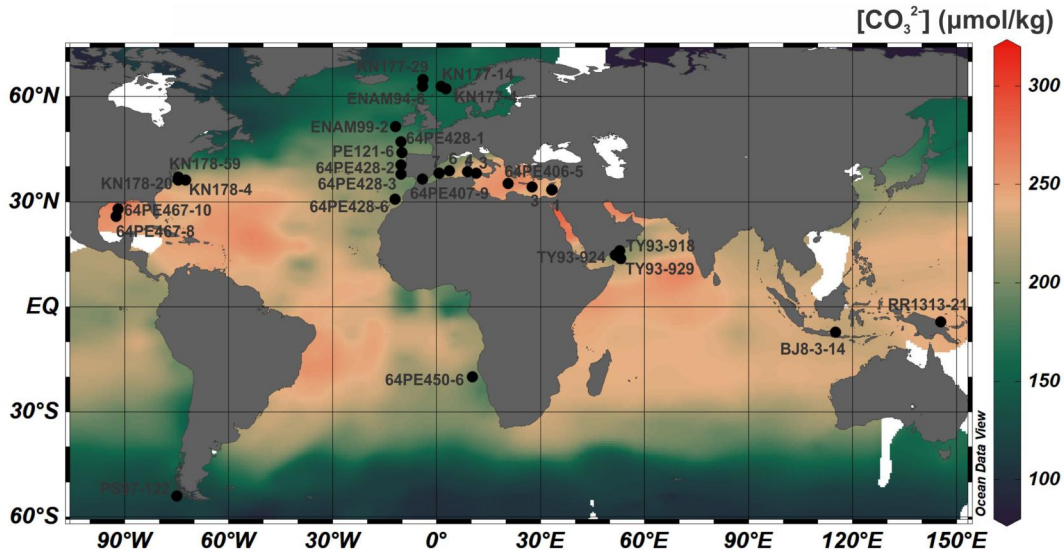

Figure 1. Sample locations of surface sediments used in this study were overlaid on mean ocean surface [CO_3^{2-}] (20 m water depth) from GLODAPv2.2022 (Lauvset et al., 2022) and SOCATv2022 (Bakker et al., 2016, 2022). The map was prepared using Ocean Data View (Schlitzer, 2022) with color palette from https://www.prafter.com/color.

2. Materials and Methods

2.1. Sample Locations and Carbonate System Parameters

In total, 30 core top (0–6 cm) sediment samples were collected from areas that span a large range of [CO_3^{2-}], [HCO_3^-], sea surface temperatures, and salinity (Figure 1). Selected sites include the coastal margin of Chile, the Gulf of Mexico, the western and eastern Atlantic Ocean, the Mediterranean Sea, the Arabian Sea, the Bali Basin and the southwestern Pacific (Table 1). All samples were of Holocene age, with descriptions and ages previously published or when not yet available, radiocarbon dated for this compilation (see Text S1 and Figure S1 in Supporting Information S1 for details) at ETH Zürich (Ausín et al., 2019; Blaauw & Christen, 2011; Wacker et al., 2013, 2014).

As samples from water overlying the core top were collected only during Mediterranean Sea cruise 64PE406, temperature, salinity, [CO_3^{2-}], [HCO_3^-] for the other sites were estimated from the SOCATv2022 (Bakker et al., 2016, 2022) and GLODAPv2.2022 data sets (Lauvset et al., 2022) using the five most proximate datapoints ($SD_{temperature}$ = 0.22–5.63°C, $SD_{salinity}$ = 0.05–3.04, $SD_{carbonate\ ion}$ = 1.70–39.3 µmol/kg, $SD_{bicarbonate\ ion}$ = 5.14–96.3 µmol/kg; shown as ±1σ SD). Due to the scarcity of carbonate system data available, only 3 data points were used to characterize the samples of TY93-918 (Arabian Sea), RR1313-21 (Bismarck Sea) and KN177, 178 at 80 m depth ($SD_{temperature}$ = 0.08–4.55°C, $SD_{salinity}$ = 0.07–0.29, $SD_{carbonate\ ion}$ = 1.88–41.4 µmol/kg, $SD_{bicarbonate\ ion}$ = 8.53–77.8 µmol/kg; shown as ±1σ SD) and one data point was used per core top sample from the western Mediterranean (64PE407). Carbonate chemistry, as well as temperature and salinity data were used from either 20 m or 80–100 m water depth corresponding to the average living depth of the planktonic foraminiferal species analyzed. Inorganic carbon chemistry of the water samples collected from the eastern Mediterranean was analyzed at the Royal Netherlands Institute for Sea Research after the expedition (Dämmer et al., 2020).

2.2. Solution Analytical Methods

Specimens of five planktonic foraminiferal species were selected: *Globigerina bulloides*, *Globigerinoides ruber ruber* (formerly known as *G. ruber pink*), *Globigerinoides ruber albus* (formerly known as *G. ruber white*), *Trilobatus sacculifer*, and *Neogloboquadrina incompta*, that are abundant and therefore, commonly used in pCO_2-reconstructions. Freeze-dried sediments were washed over a 63 µm sieve and the dried samples were further dry sieved. Specimens of every species were picked from the same size fraction to minimize the impact of ontogenetic effects. For *G. bulloides*, *G. ruber* (both), and *N. incompta*, the size fraction 150–315 µm and for *T. sacculifer*, the size fraction 315–425 µm was used. Samples were cleaned following the adapted protocol of

Table 1
Sample Locations With Corresponding Seawater Parameters (Temperature, Salinity, [CO_3^{2}], [HCO_3^{-}]) Obtained From GLODAPv2.2022 (Lauvset et al., 2022) and SOCATv2022 (Bakker et al., 2016, 2022)

Sediment core	Core depth (cm)	Latitude	Longitude	Temperature (°C)	Temperature SD (°C)	Salinity	Salinity SD	[CO_3^{2-}] (μmol/kg)	[CO_3^{2-}] SD (μmol/kg)	[HCO_3^{-}] (μmol/kg)	[HCO_3^{-}] SD (μmol/kg)
20 m											
ENAM94-06	1	62.9	−4.0	9.5	0.6	35.1	0.1	168.9	9.1	1890.1	12.1
ENAM99-02	1	51.4	−11.8	12.4	1.5	35.6	0.1	169.9	19.4	1917.6	42.4
PE121-06	1	44.0	−10.0	15.6	3.1	35.6	0.0	195.3	19.6	1857.7	47.3
64PE450-BC6	6	−20.1	10.4	23.1	1.0	35.7	0.3	218.5	13.8	1814.4	18.8
TY93-918	1	16.0	52.8	22.2	1.4	35.7	0.0	163.3	41.0	1937.6	92.2
TY93-924	1	14.7	51.6	21.7	0.6	35.7	0.1	186.7	58.2	1894.8	115.5
TY93-929	3	13.7	53.2	24.8	1.0	35.8	0.1	213.0	21.7	1825.8	52.8
64PE467-MC10	3	27.8	−91.9	26.4	4.2	35.4	1.3	240.2	14.9	1798.2	25.9
64PE467-MC08	3	25.7	−92.4	26.1	3.4	36.3	0.2	242.6	12.1	1793.7	11.1
PS97-122	0	−54.1	−74.9	8.3	2.2	33.8	0.2	125.3	18.5	1936.8	56.0
64PE407-MC09	0	36.3	−4.0	17.2		37.0		207.0		1859.0	
64PE407-MC07	0	38.0	0.7	17.0		38.0		220.0		1868.0	
64PE407-MC06	0	38.8	3.8	17.2		38.0		230.0		1900.0	
64PE407-MC04	0	38.5	9.0	16.5		38.0		248.0		1915.0	
64PE407-MC03	0	38.0	11.5	23.0		39.0		245.0		1890.0	
64PE406-MC05	0	35.0	20.6	24.7		39.0		264.7		1964.3	
64PE406-MC03	0	34.1	27.6	23.1		39.2		266.9		1965.0	
64PE406-MC01	1	33.3	33.4	23.7		39.4		243.1		2048.7	
RR1313-MC21	0	−4.3	145.5	30.0	0.1	34.1	0.1	234.6	4.0	1665.0	15.1
BJ8-03-MC14	0	−7.4	115.2	25.2	2.2	34.0	0.2	215.5	29.8	1703.1	96.3
KN178-MC59	0	36.9	−74.5	24.2	5.4	34.2	1.9	203.4	32.7	1788.2	27.6
KN178-MC04	0	36.1	−72.3	20.2	5.6	35.8	0.8	220.9	28.6	1809.2	45.3
KN178-MC20	0	36.0	−74.5	28.4	1.1	33.4	3.0	216.3	34.0	1722.6	41.2
KN177-MC14	0	62.8	1.3	10.0	4.9	34.9	0.6	152.8	27.2	1945.2	49.3
KN177-MC04	0	62.1	2.7	9.8	2.5	35.1	0.3	153.2	24.5	1936.2	47.0
KN177-MC29	0	64.8	−3.8	8.6	3.0	34.8	0.1	158.4	22.6	1908.3	53.5
64PE428-1	0	47.1	−10.2	12.0	1.1	35.6	0.1	168.3	10.2	1921.5	20.3
64PE428-2	0	40.5	−10.2	16.1	2.0	35.9	0.1	196.6	6.8	1868.5	15.1
64PE428-3	0	37.8	−10.2	17.6	0.3	36.3	0.1	210.3	1.7	1852.5	5.1
64PE428-6	0	30.7	−11.9	18.8	0.7	36.7	0.1	214.6	6.8	1871.7	12.9
80–100 m											
ENAM99-02	1	51.4	−11.8	11.9	0.2	35.6	0.0	161.2	4.5	1938.3	12.3
PE121-06	1	44.0	−10.0	12.4	0.5	35.6	0.0	169.8	5.5	1916.7	11.9
64PE407-MC04	0	38.5	9.0	16.5		38.0		248.0		2096.0	
64PE406-MC03	0	34.1	27.6	19.2		38.7		249.2		1968.1	
KN178-MC20	0	36.0	−74.5	22.4	4.6	36.4	0.3	210.8	41.4	1870.8	77.8
KN177-MC14	0	62.8	1.3	9.1	0.8	35.3	0.1	137.0	9.3	1984.2	12.9
KN177-MC04	0	62.1	2.7	8.8	0.9	35.3	0.1	141.1	1.9	1971.6	8.5
64PE428-1	0	47.1	−10.2	11.7	0.4	35.6	0.0	159.8	5.1	1941.8	13.7

Note. Seawater parameters at 20 m water depth were used for *G. bulloides*, *G. ruber* (both), *T. sacculifer* and at 80–100 m for *N. incompta*.

15252027, 2024, 4, Downloaded from https://agupubs.onlinelibrary.wiley.com/doi/10.1029/2023GC011302 by Cochrane Netherlands, Wiley Online Library on [19/04/2024]. See the Terms and Conditions (https://onlinelibrary.wiley.com/terms-and-conditions) on Wiley Online Library for rules of use; OA articles are governed by the applicable Creative Commons License

15252027, 2024, 4, Downloaded from https://agupubs.onlinelibrary.wiley.com/doi/10.1029/2023GC011302 by Cochrane Netherlands, Wiley Online Library on [19/04/2024]. See the Terms and Conditions (https://onlinelibrary.wiley.com/terms-and-conditions) on Wiley Online Library for rules of use; OA articles are governed by the applicable Creative Commons License

Barker et al. (2003). Briefly, all specimens were carefully crushed using two glass slides and transferred into acid cleaned Treff vials. Any clay particles in the samples were removed by rinsing five times with MilliQ and twice with methanol. This step was followed by the removal of organic matter. Samples were oxidized for 20 min in boiling NH_4OH-buffered 1% H_2O_2 solution, ultrasonicated, and rinsed with MilliQ four times. Any adsorbed contaminants on the shell surface were removed through the leaching of the samples with 1 mM HNO_3 and finally, all samples were dissolved in 500 µL 0.1 M ultragrade HNO_3.

Element concentrations of the shells were analyzed at the Royal Netherlands Institute for Sea Research on dissolved foraminifera using a sector-field inductively coupled plasma mass spectrometer (SF-ICP-MS, Thermo Fischer Scientific Element-2). An aliquot of 30 µL of each dissolved sample was used for pre-scanning calcium concentrations ($[Ca^{2+}]$) and all element concentrations were analyzed on matched solution $[Ca^{2+}]$. Isotopes of ^{11}B, ^{25}Mg, ^{88}Sr were measured at low resolution, whereas ^{32}S was measured at medium resolution to avoid interference of $^{16}O^{16}O$, and ^{56}Fe was analyzed at high resolution to avoid interference of $^{16}O^{40}Ar$. For all analyses, ^{43}Ca was monitored to allow calculation of elemental ratios. Element concentrations were calculated using known cosmic relative abundances. Each series of measurements included replicates except for the samples from the Arabian Sea (samples of TY93), where the limited amount of material available did not allow multiple analyses. During the analytical runs, samples alternated with 0.1 M HNO_3 for effective wash-out, and all samples were measured against 5 ratio calibration standards (de Villiers et al., 2002). For monitoring drift during the measurements, NFHS-1 (Mezger et al., 2016) standard was included and three additional standards, NFHS-2-NP (Boer et al., 2022), JCp (*Porites sp*. coral; S/Ca = 5.79 ± 0.14 mmol/mol, B/Ca = 0.50 ± 0.01 mmol/mol, Mg/Ca = 4.05 ± 0.04 mmol/mol, $\pm 1\sigma$ SD, n = 7) and JCt (*Tridacna gigas* giant clam; S/Ca = 0.57 ± 0.04 mmol/mol, B/Ca = 0.23 ± 0.01 mmol/mol, Mg/Ca = 1.21 ± 0.01 mmol/mol, $\pm 1\sigma$ SD, n = 7), provided quality control on the analysis. The internal precision of the instrument gave a relative standard deviation of 0.03%–1.88% on B/Ca, 0.06%–1.38% on Mg/Ca and 0.06%–4.30% on S/Ca ratios of the samples expressed here as $\pm 1\sigma$ RSD.

Samples were excluded from the data set when Fe/Ca values were higher than 0.2 mmol mol^{-1} (Barker et al., 2003; Regenberg et al., 2007) and/or coincided with the visible presence of pyrite precipitation on the inside or outside of the foraminifer's shell (Figure S2 in Supporting Information S1). Specimens collected from regions characterized by restricted deep water ventilation and thus low oxygen concentrations (e.g., Arabian Sea; Schenau et al., 2002) were examined under a Scanning Electron Microscope (Hitachi TM3000 SEM).

2.3. Statistical Approach

Least squares regression analysis was used to determine coefficients for linear and exponential regressions in order to evaluate the relationship between element/element ratios and various environmental parameters. The probabilities of our hypotheses were validated via significance tests, where the results are expressed as p–values, and the conventional threshold value of 0.05 is used as the significance level. Therefore, p-values lower than 0.05 are here taken as indicative of a statistically significant relationship. As not all relations can be described using linear regressions, logarithmic relations were transformed before a significance test was performed. No outliers were excluded from these tests. For the relation between S/Mg and the carbon system, confidence intervals were calculated using the bootstrap sampling technique (Rubin, 1981). The regression analysis, significance tests, and bootstrapping were executed in Python (version 3.11.2; NumPy; Scikit-learn; SciPy 1.0; Harris et al., 2020; Pedregosa et al., 2011; Virtanen et al., 2020).

2.4. Mg/Ca Analysis by LA-Q-ICP-MS

The eastern Mediterranean Sea is known to be an area where (sub)fossil foraminiferal shells are impacted by early diagenetic overgrowth, resulting in aberrant high Mg/Ca values (e.g., Boussetta et al., 2011). Therefore, we analyzed a subset of the samples, monitoring $^{25}Mg/^{44}Ca$ ratios of single shells of *G. bulloides*, *G. ruber ruber*, *G. ruber albus*, and *T. sacculifer* from the Mediterranean Sea by Laser Ablation Quadrupole Inductively Coupled Plasma Mass Spectrometry (LA-Q-ICP-MS) to identify potential inorganic overgrowth. Cleaning of this subset of foraminifera samples followed the same protocol as described in Section 2.2. For solution analysis (Barker et al., 2003), but without crushing the specimens prior to the cleaning procedure and without acid leaching and dissolution of the samples. The intact foraminifera shells were ablated from outside to inside with a circular spot of 80 µm, a repetition rate of 4 Hz, and a laser energy density of ~1 J cm^{-2}. The NIOZ Foraminifera House

15252027, 2024, 4, Downloaded from https://agupubs.onlinelibrary.wiley.com/doi/10.1029/2023GC011302 by Cochrane Netherlands, Wiley Online Library on [19/04/2024]. See the Terms and Conditions (https://onlinelibrary.wiley.com/terms-and-conditions) on Wiley Online Library for rules of use; OA articles are governed by the applicable Creative Commons License

Standard-2-Nano-Pellet (NFHS-2-NP; Boer et al., 2022) was used as a drift standard, and NIST SRM610 as a calibration standard. Data from the first 5 s of the laser ablation profile were excluded and the end condition of the profile was determined based on the increase in Al signal and 30% drop in Ca signal. Data reduction was performed using an adapted version of the MATLAB-based software package SILLS (Signal Integration for Laboratory Laser Systems; Guillong et al., 2008). The relative standard deviation of all samples for Mg/Ca ranges between 0.65% and 7.7%.

2.5. Embedding and Scanning Electron Microscopy

To investigate whether the Mg/Ca values obtained from the single foraminifera analysis (LA-Q-ICP-MS) are characteristic for the entire test or can be explained by diagenetic impact only, a cross section of one specimen was investigated using Scanning Electron Microscope (SEM). An individual test of *T. sacculifer* from the Eastern Mediterranean (64PE406-MC01) was embedded in resin (Araldite XW396/XW397) under vacuum. After the resin was fully hardened, sanding paper was used to polish the resin surface until a cross-section of the specimen was exposed. The sample surface was subsequently rinsed with MilliQ and etched twice with 0.5% HCl. After polishing and etching, the resin block was rinsed thoroughly and mounted on the adhesive surface of an SEM stub. SEM images of the cross section were obtained at an accelerating voltage of 15kV using a Hitachi TM3000 Tabletop device.

3. Results

3.1. Element Concentrations in Planktonic Foraminifera

The planktonic foraminifera measured here showed S/Ca values ranging from 0.49 to 1.8 mmol mol^{-1} with the highest ratios for *T. sacculifer* (1.0–1.8 mmol mol^{-1}) and *G. ruber ruber* (1.1–1.7 mmol mol^{-1}) and relatively large variability in *G. bulloides* (0.46–1.7 mmol mol^{-1}). B/Ca values vary between 34.6 and 212 µmol mol^{-1} with the lowest values observed for *G. bulloides* (34.6–120 µmol mol^{-1}) and the highest ratios measured in *G. ruber albus* (103–212 µmol mol^{-1}). Large intraspecies variability characterizes the Mg/Ca of all analyzed species, with values ranging from 1.5 to 18 mmol mol^{-1} in *G. bulloides*, from 0.85 to 15 mmol mol^{-1} in *N. incompta*, from 2.4 to 11 mmol mol^{-1} in *G. ruber albus*, from 3.3 to 15 mmol mol^{-1} in *G. ruber ruber* and from 2.3 to 16 mmol mol^{-1} in *T. sacculifer* (Tables 2 and 3).

3.2. High Mg/Ca Ratios

Samples from the highly saline eastern Mediterranean show noticeably elevated Mg/Ca values compared to other areas, which could (partly) obscure the overall trend between Mg/Ca and SST. Elevated Mg concentrations have been reported earlier from the Eastern Mediterranean Sea and were related to inorganic overgrowth (Ferguson et al., 2008). To account for a potential effect of overgrowths or other diagenetic impacts on foraminiferal shell chemistry, specimens of each species from the eastern Mediterranean were laser ablated to acquire Mg/Ca ratio profiles, and observed with an SEM. Inorganic calcite overgrowth can be identified by a distinct crystal morphology (Regenberg et al., 2007) that bears a modified geochemical composition compared to the original biogenic calcite signal of the foraminiferal shell (e.g., Brown & Elderfield, 1996; Coadic et al., 2013; Stainbank et al., 2020). Laser ablation profiles through the foraminiferal shells show high Mg/Ca concentrations not only in the outside coating of the foraminifera shell, but elevated values characterize the entire shell (Figure S3 in Supporting Information S1).

As samples with diagenetic overprint do not reflect the conditions in which the foraminifera grew their shells, we used the temperature, salinity and pH-based calibrations provided for foraminiferal Mg/Ca values by Gray and Evans (2019) to determine the expected species specific Mg/Ca values corresponding to the environmental parameters of the sampling location (Figure S4 in Supporting Information S1). These calibrations are available for *G. bulloides*, *T. sacculifer*, and *G. ruber albus*, and we used these to calculate Mg/Ca residuals and subsequently exclude those samples showing an offset larger than 4.5 mmol/mol compared to the expected Mg/Ca values. Although the 4.5 mmol/mol cut off is arbitrary, it clearly separates the samples deposited under regular conditions that cluster together from those from the Eastern Mediterranean that plot along a line away from this cluster. The observed large deviation in the data was obtained from the Eastern Mediterranean sites 64PE406-MC01, 64PE406-MC03, and 64PE406-MC05, and therefore samples (including also *G. ruber ruber*

Geochemistry, Geophysics, Geosystems

10.1029/2023GC011302

Table 2
Element Concentrations in G. bulloides, G. ruber ruber, G. ruber albus

	G. bulloides						*G. ruber ruber*						*G. ruber albus*					
Site	S/Ca mmol/mol	2sd mmol/mol	B/Ca µmol/mol	2sd µmol/mol	Mg/Ca mmol/mol	2sd mmol/mol	S/Ca mmol/mol	2sd mmol/mol	B/Ca µmol/mol	2sd µmol/mol	Mg/Ca mmol/mol	2sd mmol/mol	S/Ca mmol/mol	2sd mmol/mol	B/Ca µmol/mol	2sd µmol/mol	Mg/Ca mmol/mol	2sd mmol/mol
ENAM94-06	0.84	0.03	36.12	2.82	1.69	0.00												
ENAM99-02	1.33	0.10	43.97	4.63	6.06	0.08												
PE121-06	0.71	0.03	64.00	4.63	2.28	0.00												
64PE450-BC06	0.93	0.01	46.89	0.13	2.35	0.01							0.79	0.05	110.51	3.26	2.39	0.01
TY93-918	1.02	0.10	85.80	4.63	7.13	0.08							0.65	0.09	147.81	3.26	4.48	0.03
TY93-924	1.06	0.10	70.32	4.63	4.56	0.08							0.86	0.09	138.79	3.26	5.74	0.03
TY93-929	1.14	0.10	72.53	4.63	4.53	0.08							0.75	0.09	137.11	3.26	4.41	0.03
64PE467-MC10	1.67	0.10	62.18	4.63	4.18	0.08							1.41	0.07	115.00	0.85	4.39	0.01
64PE467-MC08							1.12	0.05	111.91	1.73	3.69	0.00	1.07	0.07	123.74	0.16	4.29	0.01
PS97-122	0.46	0.10	34.61	4.63	1.49	0.08												
64PE407-MC09	1.55	0.10	50.25	4.63	3.68	0.08	1.45	0.08	121.26	3.66	3.47	0.12	1.35	0.09	129.71	3.26	3.94	0.03
64PE407-MC07	1.31	0.07	49.66	1.43	4.60	0.01	1.24	0.04	122.12	2.96	5.52	0.01	1.34	0.06	114.00	1.56	4.70	0.02
64PE407-MC06	1.38	0.06	51.43	2.17	3.93	0.00	1.31	0.08	104.80	1.25	4.67	0.00						
64PE407-MC04	1.43	0.07	45.62	2.44	6.34	0.02	1.47	0.06	100.88	2.46	7.18	0.01	1.44	0.06	103.57	3.03	7.09	0.00
64PE407-MC03	1.46	0.08	45.45	0.69	4.18	0.08	1.24	0.07	124.74	3.66	4.26	0.01						
64PE406-MC05							1.48	0.08	109.45	0.44	6.46	0.12	1.61	0.07	103.40	3.18	10.63	0.03
64PE406-MC03	1.54	0.10	46.00	1.10	18.45	0.01	1.43	0.08	112.76	1.73	7.01	0.00						
64PE406-MC01							1.65	0.08	108.60	2.09	14.84	0.02	1.49	0.09	108.24	2.48	11.42	0.01
RR1313-MC21	1.72	0.10	69.50	4.65	7.51	0.08							0.97	0.09	141.73	3.26	5.65	0.03
BJ8-03-MC14	1.47	0.10	120.22	4.65	6.28	0.08							0.90	0.09	211.63	3.26	5.04	0.03
KN178-MC59	0.88	0.10	74.92	4.65	2.47	0.08	0.91	0.08	176.26	3.70	3.26	0.12						
KN178-MC04	0.75	0.10	57.94	4.65	2.20	0.08	0.83	0.08	154.02	3.70	3.99	0.12	0.81	0.09	135.97	3.26	3.86	0.03
KN178-MC20	0.81	0.10	98.84	4.65	2.66	0.08	0.80	0.08	178.88	3.70	5.54	0.12						
KN177-MC14	0.83	0.10	68.75	4.65	2.28	0.08												
KN177-MC04	0.93	0.10	99.42	4.65	2.82	0.08												
KN177-MC29	0.76	0.10	35.60	4.65	1.80	0.08												
64PE428-1	0.78	0.10	44.71	4.65	2.99	0.08												
64PE428-2	0.75	0.10	37.95	4.65	2.07	0.08												
64PE428-3	0.84	0.10	43.14	4.65	2.53	0.08												
64PE428-6	1.35	0.10	49.36	4.65	3.42	0.08	1.11	0.08	121.30	3.70	3.70	0.12						

15252027, 2024, 4, Downloaded from https://agupubs.onlinelibrary.wiley.com/doi/10.1029/2023GC011302 by Cochrane Netherlands, Wiley Online Library on [19/04/2024]. See the Terms and Conditions (https://onlinelibrary.wiley.com/terms-and-conditions) on Wiley Online Library for rules of use; OA articles are governed by the applicable Creative Commons License

15252027, 2024, 4, Downloaded from https://agupubs.onlinelibrary.wiley.com/doi/10.1029/2023GC011302 by Cochrane Netherlands, Wiley Online Library on [19/04/2024]. See the Terms and Conditions (https://onlinelibrary.wiley.com/terms-and-conditions) on Wiley Online Library for rules of use; OA articles are governed by the applicable Creative Commons License

Table 3
Element Concentrations in T. sacculifer and N. incompta

	T. sacculifer						*N. incompta*					
Site	S/Ca mmol/mol	2sd mmol/mol	B/Ca µmol/mol	2sd µmol/mol	Mg/Ca mmol/mol	2sd mmol/mol	S/Ca mmol/mol	2sd mmol/mol	B/Ca µmol/mol	2sd µmol/mol	Mg/Ca mmol/mol	2sd mmol/mol
ENAM94-06												
ENAM99-02							0.97	0.02	77.50	2.16	2.41	0.01
PE121-06												
64PE450-BC06	1.00	0.06	87.75	0.62	2.33	0.00	0.49	0.02	82.58	5.15	0.90	0.00
TY93-918												
TY93-924												
TY93-929												
64PE467-MC10	1.50	0.09	94.56	4.16	3.33	0.03						
64PE467-MC08	1.28	0.06	90.42	1.46	3.31	0.00						
PS97-122												
64PE407-MC09												
64PE407-MC07												
64PE407-MC06												
64PE407-MC04	1.61	0.05	115.15	4.16	6.15	0.01	1.15	0.08	80.00	2.62	5.80	0.02
64PE407-MC03												
64PE406-MC05	1.70	0.06	102.87	2.99	9.29	0.03						
64PE406-MC03	1.82	0.09	112.91	2.11	13.17	0.00	1.19	0.09	87.67	2.90	15.40	0.38
64PE406-MC01	1.84	0.09	108.23	1.49	16.42	0.03						
RR1313-MC21	1.14	0.09	90.68	4.16	4.52	0.03						
BJ8-03-MC14	1.25	0.09	145.71	4.16	3.75	0.03						
KN178-MC59												
KN178-MC04	0.99	0.09	101.38	4.16	3.61	0.03						
KN178-MC20							0.55	0.09	73.65	5.15	1.22	0.38
KN177-MC14							0.55	0.09	89.37	5.15	0.85	0.38
KN177-MC04							0.59	0.09	99.77	5.15	1.04	0.38
KN177-MC29												
64PE428-1							0.58	0.09	73.29	5.15	1.17	0.38
64PE428-2	0.96	0.09	87.70	4.16	2.42	0.03						
64PE428-3	1.05	0.09	89.59	4.16	2.44	0.03						
64PE428-6	1.20	0.09	99.79	4.16	2.98	0.03						

and *N. incompta*) of those stations are here excluded from further analyses and hence they are not shown on the subsequent figures.

3.3. Element/Ca Ratios Versus Sea Surface Temperature, Salinity and Carbonate System Parameters

A significant relation ($p < 0.05$) can be observed between sea surface temperature (SST) and Mg/Ca, B/Ca, or S/Ca in *G. bulloides*, where magnesium, boron and sulfur concentrations increase linearly with SST (Figure 2, Table 4). In *G. ruber ruber*, B/Ca and S/Ca show a positive and negative correlation with SST, respectively. No other species showed a significant correlation between SST and El/Ca ratios analyzed within this study.

A clear, linear correlation describes the relationship between S/Ca values and salinity only for *G. ruber ruber* ($p < 0.01$; $R^2 = 0.65$) and slightly weaker but still significant ($p < 0.05$; $R^2 = 0.17$) for *G. bulloides*. Both Mg/Ca and S/Ca of *N. incompta* correlate positively with salinity. A significant positive trend also describes the relation

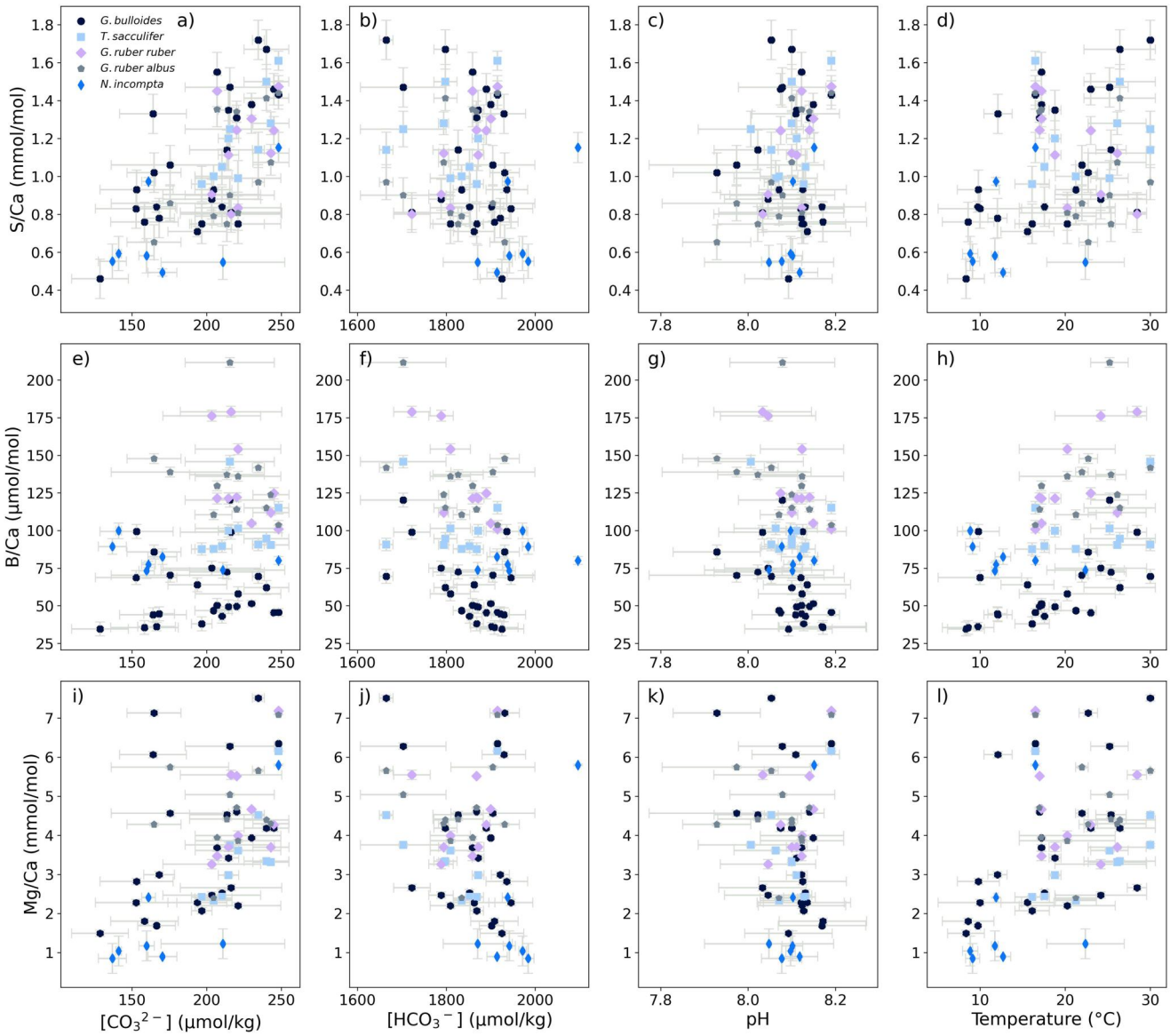

Figure 2. Ratios of sulfur (a–d), boron (e–h), and magnesium (i–l) over calcium from five planktonic foraminifera species versus carbonate system parameters ($[CO_3^{2-}]$, $[HCO_3^-]$, pH) and temperature. Error bars of the El/Ca ratios show one standard deviation of the duplicate measurements.

between seawater $[CO_3^{2-}]$ and all analyzed S/Ca values ($p < 0.001$; $R^2 = 0.43$). Considering this relationship on a species level, *G. bulloides* ($p < 0.001$; $R^2 = 0.43$), *G. ruber albus* ($p < 0.04$; $R^2 = 0.38$), as well as *T. sacculifer* ($p < 0.005$; $R^2 = 0.66$) provided a significant linear relation, while *G. ruber ruber* showed no significant relation ($p > 0.05$; $R^2 = 0.16$). Among all carbonate system parameters, Mg/Ca values are best correlated with both $[CO_3^{2-}]$ and $[HCO_3^-]$ for *N. incompta*. While the other species studied here do not show a significant relation with these parameters, the Mg/Ca values including all species linearly correlate with $[CO_3^{2-}]$ ($p < 0.001$; $R^2 = 0.28$). In all species, Mg/Ca values do not show a significant correlation with pH. Only the B/Ca values of *G. bulloides* ($p < 0.01$; $R^2 = 0.27$) and *G. ruber ruber* ($p < 0.01$; $R^2 = 0.64$) show significant negative correlations with pH and the S/Ca values of *G. ruber albus* ($p < 0.01$; $R^2 = 0.57$) and *G. ruber ruber* ($p < 0.05$; $R^2 = 0.51$) show a significant positive correlation with pH (Figure 2, Table 4).

15252027, 2024, 4, Downloaded from https://agupubs.onlinelibrary.wiley.com/doi/10.1029/2023GC011302 by Cochrane Netherlands, Wiley Online Library on [19/04/2024]. See the Terms and Conditions (https://onlinelibrary.wiley.com/terms-and-conditions) on Wiley Online Library for rules of use; OA articles are governed by the applicable Creative Commons License

Table 4
R^2 and p-Values Calculated Based on Linear Regressions Between El/Ca Ratios of G. bulloides, G. ruber ruber, G. ruber albus, N. incompta, T. sacculifer, and [CO_3^{2-}], [HCO_3^-], pH, and Temperature

	[CO_3^{2-}]		[HCO_3^-]		pH		Temperature	
	R^2	*p*-value	R^2	*p*-value	R^2	*p*-value	R^2	*p*-value
G. bulloides								
S/Ca	**0.43**	**0.00**	0.11	0.10	0.00	0.83	**0.25**	**0.01**
B/Ca	0.00	0.74	**0.23**	**0.01**	**0.27**	**0.01**	**0.25**	**0.01**
Mg/Ca	0.13	0.07	0.06	0.22	0.15	0.05	**0.24**	**0.01**
G. ruber ruber								
S/Ca	0.16	0.26	**0.70**	**0.00**	**0.51**	**0.02**	**0.50**	**0.02**
B/Ca	0.37	0.06	**0.68**	**0.00**	**0.64**	**0.01**	**0.42**	**0.04**
Mg/Ca	0.23	0.16	0.07	0.46	0.22	0.17	0.06	0.50
G. ruber albus								
S/Ca	**0.38**	**0.03**	0.01	0.79	**0.57**	**0.00**	0.14	0.23
B/Ca	0.08	0.36	0.23	0.11	0.13	0.25	0.15	0.22
Mg/Ca	0.07	0.42	0.00	0.89	0.02	0.63	0.00	0.93
N. incompta								
S/Ca	0.34	0.17	0.49	0.08	0.41	0.12	0.02	0.75
B/Ca	0.25	0.26	0.07	0.56	0.00	0.91	0.41	0.12
Mg/Ca	**0.61**	**0.04**	**0.63**	**0.03**	0.50	0.08	0.09	0.50
T. sacculifer								
S/Ca	**0.66**	**0.00**	0.01	0.76	0.14	0.28	0.01	0.83
B/Ca	0.01	0.75	0.07	0.48	0.12	0.33	0.10	0.38
Mg/Ca	**0.56**	**0.01**	0.01	0.84	0.06	0.49	0.02	0.69
All								
S/Ca	**0.43**	**0.00**	0.03	0.14	**0.07**	**0.03**	**0.09**	**0.01**
B/Ca	0.05	0.06	**0.15**	**0.00**	**0.10**	**0.01**	**0.21**	**0.00**
Mg/Ca	**0.28**	**0.00**	0.04	0.12	0.00	0.59	**0.17**	**0.00**

Note. Values are shown in bold when $p < 0.05$.

4. Discussion

4.1. Comparing El/Ca-Values Across the Complete Data Set

Overall the values observed here for Mg/Ca, B/Ca, and S/Ca are in line with previously published El/Ca data for planktonic foraminifera (Allen et al., 2012; Dämmer et al., 2020; Ferguson et al., 2008; Foster, 2008; Gray & Evans, 2019; Henehan et al., 2015; Tripati et al., 2009; Yu et al., 2007). For S/Ca, there are no previous studies reporting values for planktonic foraminifera, but the few studies on benthic species show that the S/Ca values in our data set for planktonic foraminifera are similar to those in benthic species (Van Dijk, de Nooijer, Boer, & Reichart, 2017; Van Dijk, de Nooijer, Wolthers, & Reichart, 2017).

Reconstructing paleo-temperatures is the most common application for foraminiferal Mg/Ca values (Anand et al., 2003; Dekens et al., 2002; Gray & Evans, 2019; Kısakürek et al., 2008; Lea et al., 1999; Mashiotta et al., 1999; Nürnberg et al., 1996; Saenger & Evans, 2019). For the locations and species used here, Mg/Ca correlates with temperature, but whereas previous studies impose an exponential relation, for this data set a linear correlation fits the Mg/Ca-temperature data equally well as an exponential curve (Figure S5 in Supporting Information S1). The observed high Mg/Ca values in the Eastern Mediterranean are in line with previous studies showing a progressive increase from the West to the East due to the gradual rise in salinity and calcite saturation state (Boussetta et al., 2011). These elevated Mg/Ca values are assumed to be (at least partly) associated with a post depositional diagenetic overprint, caused by the inorganic (post mortem) precipitation of calcite (Hover et al., 2001; Kozdon et al., 2013; Ni et al., 2020; Panieri et al., 2017; Sexton et al., 2006; Stainbank et al., 2020), but similar high values have been measured in shells of planktonic foraminifera collected while living from the water column during the same cruise (64PE407 and 64PE406, Dämmer et al., 2020), also indicating that not only post-depositional effects control foraminiferal Mg/Ca-values in this region (Text S2 and Figure S4 in Supporting Information S1).

Early culture experiments with planktonic foraminifera showed an effect of salinity on the shells' Mg/Ca values, suggesting a 4%–7% higher Mg concentrations for every unit increase in salinity (Dueñas-Bohórquez et al., 2009; Kısakürek et al., 2008; Lea et al., 1999; Nürnberg et al., 1996), whereas studies based on field surveys (excluding the Mediterranean Sea) showed higher salinity dependencies of 15%–27% per salinity unit (Arbuszewski et al., 2010; Mathien-Blard & Bassinot, 2009). Even higher salinity sensitivities (15%–59% per salinity unit) were reported from field studies in the Mediterranean Sea (Ferguson et al., 2008), which agrees with the results presented here (3%–60% per salinity unit).

If mainly temperature and salinity affect Mg concentrations of planktonic foraminifera, then Mg/Ca residuals calculated based on previously established temperature calibrations should correlate with seawater salinity. Mg/Ca residuals were calculated using the calibration of Mashiotta et al. (1999) for *G. bulloides* ($Mg/Ca = 0.47 \pm 0.03*\exp^{0.108\pm0.003*T}$), the calibration of Dekens et al. (2002) for *T. sacculifer* ($Mg/Ca = 0.37 \pm 0.03*\exp^{0.09\pm0.013*T}$) and the corresponding calibrations of Anand et al. (2003) for *G. ruber ruber* ($Mg/Ca = 0.381 \pm 0.01*\exp^{0.09*T}$) and *G. ruber albus* ($Mg/Ca = 0.449 \pm 0.006*\exp^{0.09*T}$). In accordance with former observations on the salinity dependence of Mg incorporation, residuals for Mg/Ca values in this study also depend on salinity. Still, a highly significant correlation ($p < 0.05$ for each species) is also observed between Mg/Ca residuals and seawater [HCO_3^-] values based on a linear regression test (Figure 3). Residual Mg/Ca values of only *T. sacculifer* and *G. ruber albus* show slightly better correlation with salinity than with [HCO_3^-], while *G. ruber ruber* does not show a significant relationship ($p > 0.05$) with salinity. However, because seawater salinity and [HCO_3^-] co-vary inherently in nature, our study is not suitable for deconvolving these effects. Culture

15252027, 2024, 4, Downloaded from https://agupubs.onlinelibrary.wiley.com/doi/10.1029/2023GC011302 by Cochrane Netherlands, Wiley Online Library on [19/04/2024]. See the Terms and Conditions (https://onlinelibrary.wiley.com/terms-and-conditions) on Wiley Online Library for rules of use; OA articles are governed by the applicable Creative Commons License

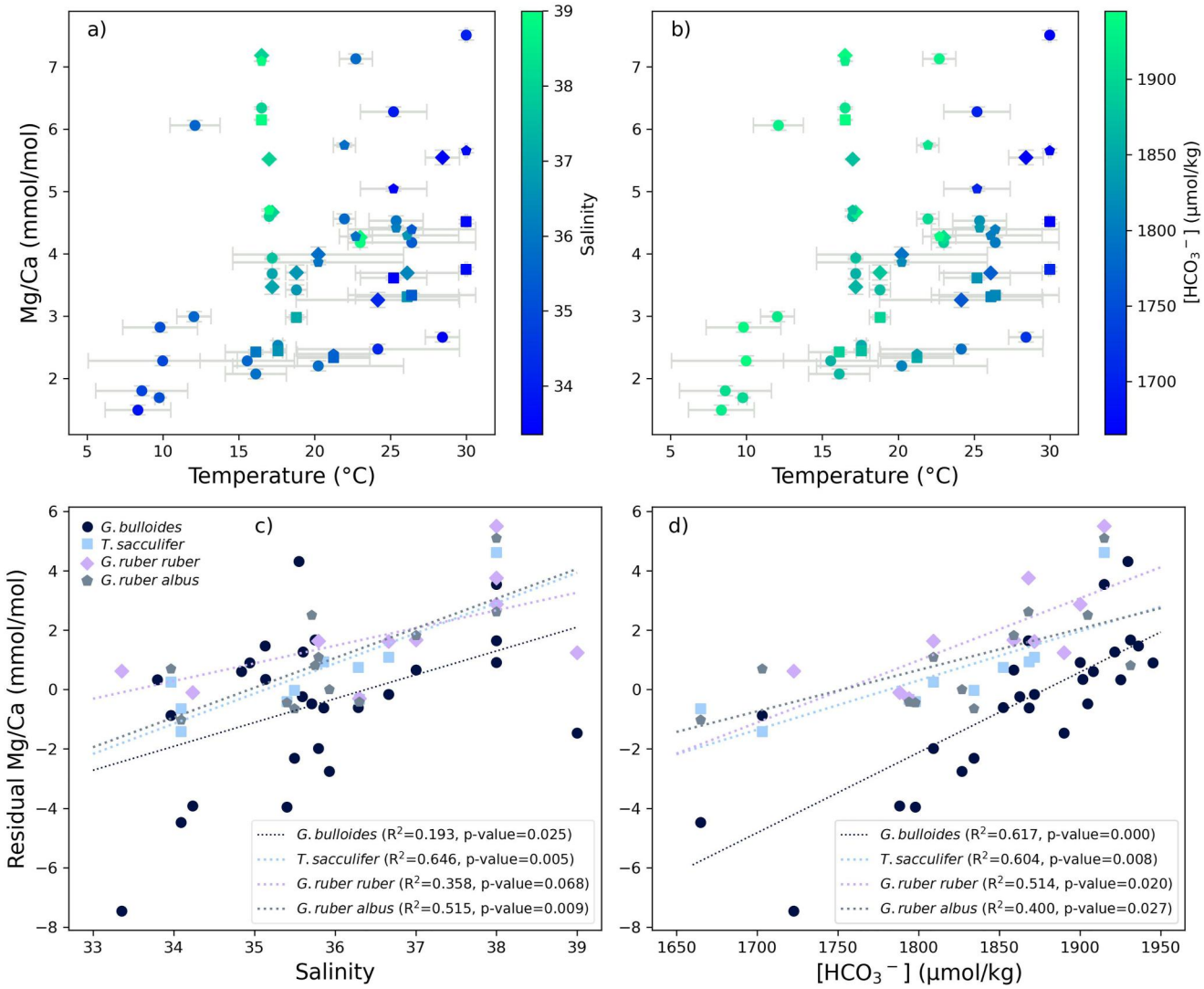

Figure 3. The top panels show Mg concentrations plotted against sea surface temperature at 20 m depth for *G. bulloides*, *G. ruber ruber*, *G. ruber albus*, and *T. sacculifer* with (a) salinity, (b) [HCO_3^-] color codes. The bottom panels display residuals of Mg/Ca based on Mg/Ca—temperature calibrations (Anand et al., 2003; Dekens et al., 2002; Mashiotta et al., 1999) and plotted against (c) salinity and (d) [HCO_3^-]. The corresponding temperature, salinity and [HCO_3^-] data were obtained from the GLODAPv2.2022 (Lauvset et al., 2022) and SOCATv2022 (Bakker et al., 2016, 2022) data sets.

experiments with controlled seawater carbon chemistry already stressed the influence of the carbonate system on the incorporation of magnesium, although these studies mainly focused on the effect of pH (Gray et al., 2018; Lea et al., 1999) and [CO_3^{2-}] (Arbuszewski et al., 2010; Khider et al., 2015; Russell et al., 2004) and did not decouple it from the potential influence of [HCO_3^-]. Calculating once more residuals, now from the relation found between the temperature-based residual Mg/Ca and salinity, indicates a remaining dependency on carbon chemistry (e.g., Gray et al., 2018) caused by seawater [HCO_3^-] rather than by pH (Figure S6 in Supporting Information S1).

For all foraminiferal species we studied, the range of B/Ca values are comparable to previously published data (Foster, 2008; Henehan et al., 2015; Krupinski et al., 2017; Yu et al., 2007), but they do not vary in accordance with previously proposed [CO_3^{2-}] and pH calibrations. Also, especially for *G. bulloides*, intraspecies variability is large in the core-top B/Ca values of this study compared to the observations of Yu et al. (2007) and Krupinski et al. (2017) (Figure S7 in Supporting Information S1). Culture experiments with varying pH reported more boron incorporated at higher pH (Allen et al., 2012; Henehan et al., 2015), which is an opposite trend compared to what is found here. Core-top results from Henehan et al. (2015), however, showed a negative or no correlation between B/Ca and pH, similar to our field study. Such inconsistencies suggest that foraminiferal B/Ca values depend on

15252027, 2024, 4, Downloaded from https://agupubs.onlinelibrary.wiley.com/doi/10.1029/2023GC011302 by Cochrane Netherlands, Wiley Online Library on [19/04/2024]. See the Terms and Conditions (https://onlinelibrary.wiley.com/terms-and-conditions) on Wiley Online Library for rules of use; OA articles are governed by the applicable Creative Commons License

15252027, 2024, 4, Downloaded from https://agupubs.onlinelibrary.wiley.com/doi/10.1029/2023GC011302 by Cochrane Netherlands, Wiley Online Library on [19/04/2024]. See the Terms and Conditions (https://onlinelibrary.wiley.com/terms-and-conditions) on Wiley Online Library for rules of use; OA articles are governed by the applicable Creative Commons License

more than one environmental parameter that in addition might also include variations induced by symbionts (Osborne et al., 2020). The relationship between B/Ca and pH found here and in previous studies likely results from confounding factors playing a smaller or larger role. Therefore, one may expect larger intraspecies variability of B/Ca values in a globally extended field survey than in a regional core-top study.

Besides the multiple environmental parameters, seawater chemistry may need to be constrained as concentrations and aqueous speciation of elements, such as calcium and magnesium, may impact the incorporation of another (Haynes et al., 2017, 2019). The influence of variation in seawater chemistry on the incorporation of elements may be constrained through inorganic calcite growth experiments (e.g., Uchikawa et al., 2017), but differences in precipitation rates at which the foraminiferal and inorganic calcites are grown complicate the comparison of these studies (Haynes et al., 2017). Among the potential multiple controls on boron incorporation, the carbon system may be a primary one. However, results of this and previous studies indicate that the application of B/Ca as a proxy may be limited to times when the seawater chemistry is well constrained and may need to be applied along with multiple elements to resolve uncertainties derived from various environmental parameters.

4.2. Evaluation of S/Ca as a Proxy for $[CO_3^{2-}]$

The direction of the S/Ca-$[CO_3^{2-}]$ relationship we observed in core top samples for planktonic foraminifera is inverted compared to the relationship found in a culturing experiment using benthic foraminifera (Van Dijk, de Nooijer, Boer, & Reichart, 2017; Van Dijk, de Nooijer, Wolthers, & Reichart, 2017). In the field study presented here, the primary influence of $[CO_3^{2-}]$ may, however, be masked by the effects of other environmental parameters that are anti-correlated under natural conditions. Moreover, covariance between the parameters of the carbonate system and also between the carbonate system parameters and salinity potentially complicates isolating the effect of a single parameter on S incorporation.

To test this, we corrected for the influences of other parameters on the $[CO_3^{2-}]$-S/Ca relationship by using linear regressions for S/Ca with either temperature, salinity, or Mg/Ca. The residuals of these three regression analyses, however, did not correlate with $[CO_3^{2-}]$ (Figure S8 in Supporting Information S1). This implies that the incorporation of sulfur in $CaCO_3$ is either affected by a parameter not directly coupled to the marine inorganic carbon system, or by one or more parameters not considered here. In controlled culture experiments of benthic foraminifera where temperature, salinity, and pH were kept constant, sulfur incorporation was negatively correlated with $[CO_3^{2-}]$ (Van Dijk, de Nooijer, Boer, & Reichart, 2017; Van Dijk, de Nooijer, Wolthers, & Reichart, 2017). However, in the experiments conducted so far, $[CO_3^{2-}]$ covaried with DIC, $[HCO_3^{-}]$, and alkalinity. Fully decoupling all components of the CO_2 system could pinpoint the controls of the carbonate system on S incorporation. Within and between the species studied, Mg/Ca and S/Ca values are positively correlated (Figure 4) and alternatively, the positive correlation between Mg/Ca and S/Ca can be used to constrain the effect of the inorganic carbon system (and $[CO_3^{2-}]$ in particular) on sulfur incorporation.

To compensate for the observed strong coupling of Mg/Ca and S/Ca, we are here exploring the ratio of sulfur and magnesium (S/Mg) and its dependency on environmental parameters. The relatively large scatter in S/Mg ratios observed for *G. bulloides* when plotted against $[CO_3^{2-}]$ may be caused by the large genetic variability of this species (Darling & Wade, 2008; Sadekov et al., 2016) in combination with the large geographical span of the samples, that might cause appreciable scatter. *G. bulloides* is present over a wide range of environmental conditions, with the same morphological appearance, but different, genotype-dependent, geochemical signatures. The largest genetic diversity is identified in (sub-)tropical regions (Rutherford et al., 1999), where seasonal changes in the hydrographic regime may control the foraminiferal assemblages (Kincaid et al., 2000). Although the inorganic carbon chemistry data were averaged to minimize seasonal bias, we cannot exclude the possibility that a mismatch between genotypes of *G. bulloides* and the carbon chemistry data set may result in an offset between El/Ca ratios and $[CO_3^{2-}]$ (Steinke et al., 2005).

The two locations from the Arabian Sea, which were not compromised by the presence of pyrite, still show an offset compared to the overall trend. The Arabian Sea is known for the large intra-annual change in surface water carbon chemistry related to upwelling and the data here used for surface water carbon chemistry relate to the non-upwelling season, whereas the specimens most likely rather grew during the high productive upwelling season. Rather than trying to back-correct these data points to the upwelling season, for which data are not accessible, we decided to omit them from further statistical analyses.

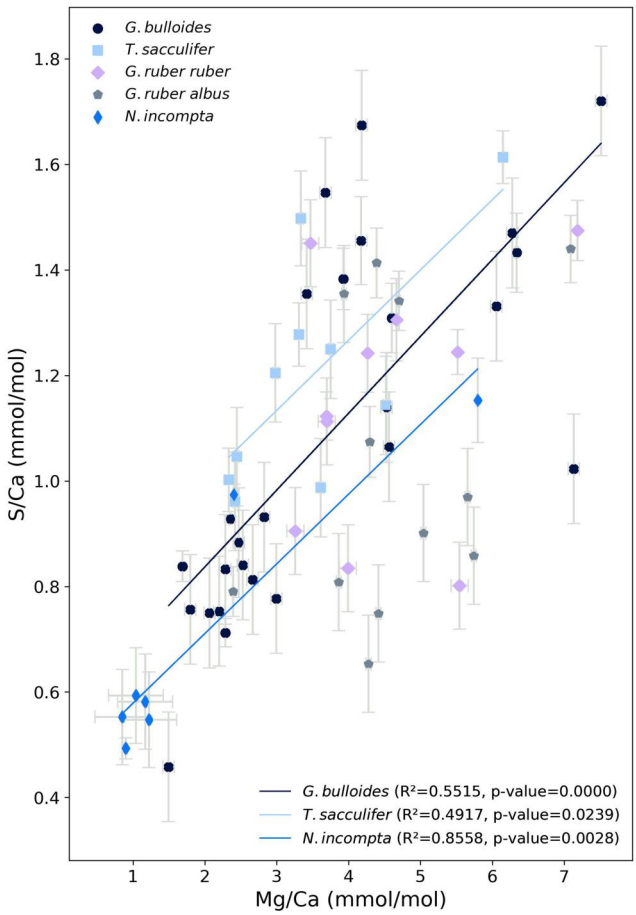

Figure 4. Foraminiferal S/Ca values versus Mg/Ca values fitted with linear regression lines. Regression lines are not shown for the species when $p > 0.05$. Error bars on S/Ca and Mg/Ca values are expressed as $\pm 1\sigma$ uncertainties derived from duplicate analysis of the samples.

After excluding the *G. bulloides* and the Arabian Sea derived data points, the multi-species's ratio of sulfur and magnesium (S/Mg) values versus seawater [CO_3^{2-}] show a significant linear correlation ($p < 0.00001$, $R^2 = 0.52$) when it is evaluated over the large range in seawater [CO_3^{2-}] values that were investigated here including the four species, *G. ruber ruber*, *G. ruber albus*, *N. incompta* and *T. sacculifer* (Figure 5). The linear relationship is evident due to the high S/Mg ratios of *N. incompta*, and further studies filling in the gap of [CO_3^{2-}] between *N. incompta* and the other species studied here (*G. ruber ruber*, *G*, *ruber albus*, *T. sacculifer*) are needed to improve this relation. One may expect the residuals to show the same identical correlation as taking the ratio of S over Mg. However, as the calculations for the residuals are based on re-described relationships, small offsets are translated in added noise. By directly taking the ratio of these elements, we do not prescribe any relation and the correlation between the ratio as actually measured on the foraminiferal carbonate is directly cross correlated with seawater chemistry. Because the relationship is not very strong (R^2 is only 0.52), added noise readily obscures this relationship.

The observed correlation provides an outlook into a new potential carbonate chemistry proxy, but also relies on understanding the coupling of the incorporations of sulfur and magnesium, both somehow being affected by linked processes and thus combining shared control(s). Based on earlier studies investigating the controls on foraminiferal Mg/Ca, we may suspect, for instance, an influence of salinity, growth rate, and potentially of temperature, whereas the control of [CO_3^{2-}] on the incorporation of both S (Van Dijk, de Nooijer, Boer, & Reichart, 2017; Van Dijk, de Nooijer, Wolthers, & Reichart, 2017) and Mg (Elderfield et al., 2006; Rosenthal et al., 2006; Russell et al., 2004) has been validated before using culture experiments and field studies. The calibration of Van Dijk, de Nooijer, Wolthers, and Reichart (2017) and Van Dijk, de Nooijer, Boer, and Reichart (2017) was based on high-Mg benthic foraminifera, which potentially has a different calcification pathway and moreover, the incorporation of various ions may also influence each other (Mewes et al., 2015).

4.3. A Mechanistic Link Between Mg- and S-Incorporation

The incorporation of one ion may affect the incorporation of another one, hence indirectly linking an environmental parameter to incorporate an ion or element in the foraminiferal shell carbonate. Mg/Ca and S/Ca, for example, are positively correlated with foraminiferal calcite across multiple spatial scales. Benthic species incorporating relatively much Mg also have higher S/Ca (Van Dijk et al., 2019). This positive correlation between the two elements can also be observed within the planktonic species we studied: this relation is the most significant for *G. bulloides* ($p < 0.0001$, $R^2 = 0.55$) but a significant positive correlation ($p < 0.0001$, $R^2 = 0.43$) was also observed when combining all planktonic foraminifera species studied here (Figure 4). Within a single chamber wall, the distribution of Mg and S are also positively correlated (Geerken et al., 2019; Van Dijk et al., 2019), both occurring in bands of elevated concentrations parallel to the outer and inner surface and in close proximity to the primary organic sheet (i.e., where the first layers of a chamber wall are precipitated). The correlation between S and Mg at the inter-species, intra-species and intra-specimen levels suggests that the incorporation of these two elements is somehow mechanistically coupled.

The ionic radius of Mg^{2+} is smaller than that of the Ca^{2+} and therefore, substitution of Ca^{2+} by Mg^{2+} induces a tension in the structure of the calcite lattice (Evans, 1966; Maslen et al., 1995). Accordingly, the incorporation of Mg^{2+} may facilitate the incorporation of larger ions, which would compensate for the distorted crystal lattice. Ions such as SO_4^{2-} would by themselves stretch the calcite lattice (Fernández-Díaz et al., 2010; Kontrec et al., 2004; Okumura et al., 2018), but incorporated SO_4^{2-} also results in the rotation of the adjacent CO_3^{2-} groups and a

15252027, 2024, 4, Downloaded from https://agupubs.onlinelibrary.wiley.com/doi/10.1029/2023GC011302 by Cochrane Netherlands, Wiley Online Library on [19/04/2024]. See the Terms and Conditions (https://onlinelibrary.wiley.com/terms-and-conditions) on Wiley Online Library for rules of use; OA articles are governed by the applicable Creative Commons License

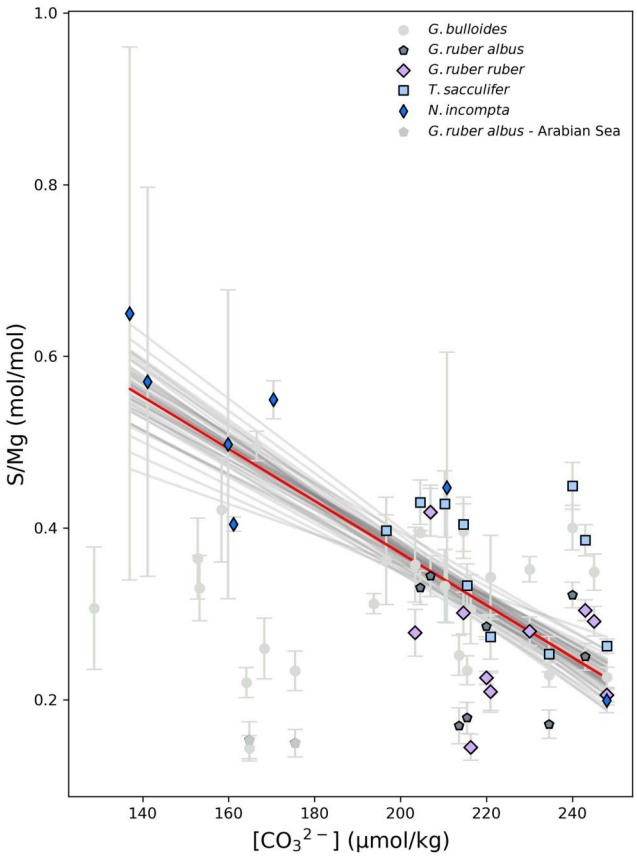

Figure 5. S/Mg ratios of *G. bulloides*, *G. ruber albus*, *G. ruber ruber*, *T. sacculifer*, and *N. incompta* versus [CO_3^{2-}] with bootstrap confidence interval. *G. bulloides* and the samples from the Arabian Sea are not included in the bootstrap test.

more prominent displacement of Ca^{2+} due to the stretched apical oxygen of the SO_4^{2-} anion. Therefore, carbonates with high Mg concentrations could potentially accommodate more sulfate ions (Takano, 1985).

During the calcite formation, enhanced uptake of magnesium ions is known to coincide with elevated incorporation of other elements as well (Kunioka et al., 2006; Mewes et al., 2015; Okumura & Kitano, 1986). During calcite crystal growth, blocking of kink sites and formation of nonequivalent surfaces will not only cause a higher affinity for Mg^{2+} to attach (Paquette et al., 1996) but also promote overall trace element partitioning (Paquette & Reeder, 1990). Staudt et al. (1994) showed that the same surface structural forces influence the incorporation of anionic complexes.

Magnesium ions may be promoting sulfate incorporation via its difference in crystallographic unit size radius as explained above, or the co-variance of Mg/Ca and S/Ca may be indirect due to an impact on both via for example, crystal growth rate. Such relations between Mg^{2+} and SO_4^{2-} would imply a proportional increase when both anions and cations are available. The samples from the Eastern Mediterranean showed elevated Mg concentrations while the S/Ca values did not linearly follow this increase (Figure S9 in Supporting Information S1). As diagenesis may affect these samples, sulfur concentrations are either less susceptible to overgrowth, or diagenesis imposes a reduction in S/Ca. However, these observations may also indicate that the lattice distortion arising from the smaller ionic radius of Mg may not be the primary cause for the preferred SO_4^{2-} substitution for CO_3^{2-}. This observation agrees with the results from previous studies on elemental banding within the foraminiferal chamber walls (Van Dijk et al., 2019) showing a spatial correlation between S and Mg but also a partial decoupling of their concentrations. This may indicate that the elevated S/Ca values observed are partly related to Mg^{2+} incorporation and also partly to shared impacts of environmental parameters, such as elevated saturation state.

A supersaturation in sulfur uptake could derive from the capacity of the calcite lattice to host anions with larger ionic radius, and hence provide a threshold for the shell's S/Ca. This would imply that S/Ca ratios should level off at a critical concentration, at the same time depending on the Mg uptake. Substitution of impurities for either Ca^{2+} or CO_3^{2-} may not have an identical influence on growth rate. The effect on the growth rate will vary not just based on which anion or cation substitutes, but the incorporated concentrations may also induce changes in the growth rate (Nielsen et al., 2013). Thus, a threshold could exist for the incorporation of sulfur as well that would create a transport limitation for sulfur when it diffuses to the mineral surface. Alternatively, the limitation of sulfur incorporation could be linked to the Mg/Ca values. High Mg concentrations contribute to morphological changes in the original calcite lattice, as indicated by the formation of roughened growth step sites in inorganically precipitated calcites (Davis et al., 2004). Such a drastic change in calcite surface chemistry and hence morphology may become unfavorable for incorporating the SO_4^{2-} ions (Midgley et al., 2021) and thus results in a decoupling of the otherwise linear co-variance of sulfur and magnesium.

4.4. Competition of Ions During Incorporation Into the Crystal Lattice

Early studies investigating sulfur concentrations in carbonates showed that sulfur is primarily incorporated into $CaCO_3$ in the form of sulfate (Pingitore et al., 1995, 1997) by substituting for CO_3^{2-} in the crystal lattice. In general, the structural suitability and the chemical speciation in which the element is present determine the capacity of substitution for CO_3^{2-}. However, not only isostructural oxyanions could compete with SO_4^{2-} for a CO_3^{2-}-position in the crystal lattice, but a carbonate ion may also be replaced by anions of U (Keul et al., 2013; Raitzsch et al., 2011; Russell et al., 2004), Zn (Van Dijk, de Nooijer, Boer, & Reichart, 2017; Van Dijk, de

15252027, 2024, 4, Downloaded from https://agupubs.onlinelibrary.wiley.com/doi/10.1029/2023GC011302 by Cochrane Netherlands, Wiley Online Library on [19/04/2024]. See the Terms and Conditions (https://onlinelibrary.wiley.com/terms-and-conditions) on Wiley Online Library for rules of use; OA articles are governed by the applicable Creative Commons License

15252027, 2024, 4, Downloaded from https://agupubs.onlinelibrary.wiley.com/doi/10.1029/2023GC011302 by Cochrane Netherlands, Wiley Online Library on [19/04/2024]. See the Terms and Conditions (https://onlinelibrary.wiley.com/terms-and-conditions) on Wiley Online Library for rules of use; OA articles are governed by the applicable Creative Commons License

Nooijer, Wolthers, & Reichart, 2017) or B (e.g., Brown et al., 2011; Rae et al., 2011; Yu & Elderfield, 2007). Hence, the ratios of such elements in the shell may also reflect the seawater carbonate ion concentration.

Structural preference will determine which anion may take the position in the calcite lattice. For instance, borate ($B(OH)_4^-$) substitutes for CO_3^{2-} (Hemming & Hanson, 1992) in $CaCO_3$, and therefore, the changing marine inorganic carbon chemistry will challenge both SO_4^{2-} and $B(OH)_4^-$ to attempt the incorporation for the same calcite lattice position. Boron is, however, present in seawater in very low concentrations compared to sulfate and accordingly is also incorporated as a trace element only and will therefore not compete as such with SO_4^{2-}.

Inorganic calcite precipitation experiments showed that in addition to $B(OH)_4^-$, boric acid ($B(OH)_3$) may also be incorporated into calcite (e.g., Uchikawa et al., 2015) and the amount of $B(OH)_3$ uptake is potentially following a growth rate pattern (Farmer et al., 2019). A positively charged calcite surface promotes the incorporation of the negatively charged borate ion; however, its tetrahedral configuration can be fitted into the trigonal space only after its transformation (Branson et al., 2015; Hemming et al., 1998; Klochko et al., 2009; Ruiz-Agudo et al., 2012; Sen et al., 1994). Sulfate may not undergo a coordination change prior to the substitution for CO_3^{2-} (Busenberg & Plummer, 1985; Staudt et al., 1994), but its incorporation requires a lattice adjustment due to its larger size compared to CO_3^{2-} (Goetschl et al., 2019; Kontrec et al., 2004).

As the incorporation of SO_4^{2-} inhibits calcite precipitation (Pokroy et al., 2006), this anion may provide a more suitable surface for the attachment of $B(OH)_3$. This would imply that S concentrations would allow correcting such growth rate effects for boron (and vice versa).

Early studies on boron incorporation reported a linear correlation between the foraminifera's B/Ca values and the seawater $[CO_3^{2-}]$ (Brown et al., 2011; Rae et al., 2011; Yu & Elderfield, 2007). Similar to S/Ca, B/Ca may not be applicable as a proxy for $[CO_3^{2-}]$ as potentially more than only one parameter affects boron incorporation (Allen et al., 2011; Henehan et al., 2015; Uchikawa et al., 2023). Dependency on multiple environmental parameters may regulate the incorporation of these anions and thus correcting for the effect of one of those parameters may allow isolating the change in another and this way to establish a more robust reconstruction method for one parameter only.

4.5. Toward Improved Marine Carbon System Reconstructions

Uncertainties in the Mg/Ca-paleothermometer prompted attempts to improve the method by combining foraminiferal Mg/Ca data with Sr/Ca (Dissard et al., 2021; Lea et al., 1999; Reichart et al., 2003; Russell et al., 2004). Because Mg/Ca values are not always related to temperature in aragonitic foraminifera and especially corals (Bryan & Marchitto, 2008; Fallon et al., 2003), lithium and magnesium concentrations were combined (Li/Mg), similarly in an attempt to improve reconstructions of past seawater temperature (Case et al., 2010; Cuny-Guirriec et al., 2019; Fowell et al., 2016; Hathorne et al., 2013; Montagna et al., 2014; Raddatz et al., 2013). Also, B was ratioed with Mg as proposed by Wu et al. (2021) using B/Mg values of corals as a new proxy for sea surface temperature, as they demonstrated that both Li/Mg and B/Mg have a stronger correlation with temperature than Mg concentrations alone.

Using the S/Mg ratio as a proxy for $[CO_3^{2-}]$ aims at correcting for a joint common factor, thereby isolating the impact of carbonate ion concentration. One of the potential mechanisms behind the observed correlation might involve the precipitation rate during chamber formation. As the rate of calcification may correlate with seawater $[CO_3^{2-}]$ (i.e., calcite saturation state), a positive correlation between S/Ca and $[CO_3^{2-}]$ could reflect the (indirect) effect of precipitation rate. The growth by a foraminifer, that is, chamber addition rate, is not necessarily reflecting calcite crystal precipitation rate; therefore, it may be that an individual who completes its life cycle in a week, precipitates its calcite at the same rate as an individual who gradually adds its chambers over a whole year. Since the actual calcite precipitation rates in foraminifera are constrained for a single species alone (Geerken et al., 2022), it remains to be tested whether chamber addition rates are correlated with precipitation rates as they are recorded in inorganic precipitation experiments. Precipitation rates may also vary with ontogeny (Ni et al., 2007), potentially explaining the elemental variability related to specimen's size (e.g., Mg and Sr; Babila et al., 2014; Elderfield et al., 2002). Comparison of calcite chemistry from specimens selected from a relatively narrow size fraction in this study aimed to minimize the potential effect of size or ontogeny through precipitation rate.

15252027, 2024, 4, Downloaded from https://agupubs.onlinelibrary.wiley.com/doi/10.1029/2023GC011302 by Cochrane Netherlands, Wiley Online Library on [19/04/2024]. See the Terms and Conditions (https://onlinelibrary.wiley.com/terms-and-conditions) on Wiley Online Library for rules of use; OA articles are governed by the applicable Creative Commons License

Results from inorganic calcite growth experiments suggest that the precipitation rate may influence sulfur incorporation (Busenberg & Plummer, 1985); however, comparing inorganic and foraminiferal calcite in such a way is confined by the differences in precipitation rates. If the S/Ca values of this study were strongly influenced by the calcification rate, this would likely be reflected by other element ratios too (e.g., Sr; Cléroux et al., 2008; Keul et al., 2017; Kısakürek et al., 2008). Since we did not find a significant correlation between S and Sr in four of the five species studied here and only a slight covariance in the one species, *G. bulloides* ($p < 0.05$, $R^2 = 0.33$) based on a linear regression test (Figure S10 in Supporting Information S1), it appears unlikely that differences in precipitation rate by itself caused the observed variability in foraminiferal S/Ca.

The earlier mentioned approaches to combine multiple elements fundamentally attempt, each with its own inherent confounding factors affecting their incorporation in the foraminiferal test carbonate, to better resolve either temperature or carbonate system parameters. Accordingly, we here suggest focusing future work on combining multiple elements to better constrain the marine inorganic carbon chemistry and to correct for the influence of different partly unknown factors, of which they share the impact on their incorporation. For instance, calcite growth experiments indicated that some of the elements incorporated into the foraminiferal shells are affected by the rate of precipitation. As there is no available proxy to detect the calcite precipitation rate of foraminifera, the use of multiple elements can potentially correct for this parameter and isolate the influence of other factors such as carbon chemistry, temperature, or salinity. Analytical advances now allow for many elements to be measured simultaneously on a small volume of foraminiferal material. This in turn, provides the opportunity to combine various element-environmental relationships and correct for potential multi-factor effects of a single environmental parameter on multiple elements (and vice versa, e.g. Marchitto, 2006; Yu et al., 2005). By combining several elements in a multifactor calibration it should accordingly be possible to deconvolve and constrain the different factors involved, provided that for enough of these elements the fundamental chemistry is understood. With the multielement calibration presented here we hope to make a first step toward such an approach.

5. Conclusions

Ratios of S/Ca, Mg/Ca, and B/Ca were measured in five planktonic foraminifera species from core-tops that cover a wide range of carbonate system conditions ($[CO_3^{2-}]$, $[HCO_3^-]$, pH), temperatures and salinities. Sulfur concentrations positively correlate with the seawater's $[CO_3^{2-}]$, which is opposite compared to previous results based on benthic foraminiferal culture experiments. These results indicate that a potential impact of $[CO_3^{2-}]$ on the incorporation of sulfur in planktonic foraminifera may be overwritten by one or more other factors. Similarly, we investigated secondary controls on the Mg incorporation in addition to temperature that may influence the primary temperature effect. Residual analysis of the Mg/Ca values indicates a more significant correlation with the seawater's $[HCO_3^-]$, potentially even stronger than the impact of salinity. Also, a strong positive correlation was observed between S and Mg, which may or may not be linked to changes in carbonate system parameters as well. Nonetheless, their strong covariation hint to (a) common process(es) being responsible for the incorporation of both these elements. Combining these elements in a S/Mg ratio, canceling out these common factors we observe a strong correlation to seawater carbonate ion concentration. This shows the potential of using multiple elements to isolate the influence of one parameter of the carbon system while correcting for shared environmental controls. A multi-element approach may also resolve uncertainties derived from yet unconstrained parameters on the El/Ca incorporations in the foraminifera shells.

Data Availability Statement

Single foraminifera Mg/Ca ratios are available through the NIOZ Data Archive System at https://doi.org/10.25850/nioz/7b.b.5g (Karancz et al., 2024).

Acknowledgments
This work was carried out under the program of the Netherlands Earth System Science Centre (NESSC), financially supported by the Ministry of Education, Culture and Science (OCW) and the European Union's Horizon 2020 research and innovation program under the Marie Skłodowska-Curie Grant 847504. We also acknowledge support from NSF Grant OCE-1834208 to YR. We thank Jelle Bijma and Frank Lamy for providing samples from the Chilean Margin. We are grateful for the technical support with the geochemical analysis to Patrick Laan and Wim Boer, for the assistance with sediment core preparation to Piet van Gaever, and for the support of the laboratory of Ion-Beam Physics at ETH Zurich. We thank the editor and two reviewers, Anne Gothmann and one anonymous reviewer, whose comments greatly impoved the manuscript. We wish to acknowledge Steven van Heuven and Karel Bakker for providing carbon chemistry data from cruise 64PE406 and special thanks to Matthew Humphreys for processing the obtained carbon chemistry data.

References

Allen, K. A., & Hönisch, B. (2012). The planktic foraminiferal B/Ca proxy for seawater carbonate chemistry: A critical evaluation. *Earth and Planetary Science Letters*, *345–348*, 203–211. https://doi.org/10.1016/j.epsl.2012.06.012

Allen, K. A., Hönisch, B., Eggins, S. M., & Rosenthal, Y. (2012). Environmental controls on B/Ca in calcite tests of the tropical planktic foraminifer species *Globigerinoides ruber* and *Globigerinoides sacculifer*. *Earth and Planetary Science Letters*, *351*, 270–280. https://doi.org/10.1016/j.epsl.2012.07.004

Allen, K. A., Hönisch, B., Eggins, S. M., Yu, J., Spero, H. J., & Elderfield, H. (2011). Controls on boron incorporation in cultured tests of the planktic foraminifer *Orbulina universa*. *Earth and Planetary Science Letters*, *309*(3–4), 291–301. https://doi.org/10.1016/j.epsl.2011.07.010

Anand, P., Elderfield, H., & Conte, M. H. (2003). Calibration of Mg/Ca thermometry in planktonic foraminifera from a sediment trap time series. *Paleoceanography*, *18*(2), 1050. https://doi.org/10.1029/2002pa000846

Arbuszewski, J., de Menocal, P., Kaplan, A., & Farmer, E. C. (2010). On the fidelity of shell-derived $\delta^{18}O_{seawater}$ estimates. *Earth and Planetary Science Letters*, *300*(3–4), 185–196. https://doi.org/10.1016/j.epsl.2010.10.035

Ausín, B., Haghipour, N., Wacker, L., Voelker, A. H. L., Hodell, D., Magill, C., et al. (2019). Radiocarbon age offsets between two surface dwelling planktonic Foraminifera species during abrupt climate events in the SW Iberian margin. *Paleoceanography and Paleoclimatology*, *34*(1), 63–78. https://doi.org/10.1029/2018pa003490

Babila, T. L., Rosenthal, Y., & Conte, M. H. (2014). Evaluation of the biogeochemical controls on B/Ca of *Globigerinoides ruber* white from the oceanic flux program, Bermuda. *Earth and Planetary Science Letters*, *404*, 67–76. https://doi.org/10.1016/j.epsl.2014.05.053

Bakker, D. C., Alin, S. R., Becker, M., Bittig, H. C., Castaño-Primo, R., Feely, R. A., et al. (2022). *Surface ocean CO_2 atlas database version 2022 (SOCATv2022) (NCEI accession 0253659)*. NOAA National Centers for Environmental Information. https://doi.org/10.25921/1h9f-nb73

Bakker, D. C., Pfeil, B., Landa, C. S., Metzl, N., O'brien, K. M., Olsen, A., et al. (2016). A multi-decade record of high-quality fCO_2 data in version 3 of the Surface Ocean CO_2 Atlas (SOCAT). *Earth System Science Data*, *8*(2), 383–413. https://doi.org/10.5194/essd-8-383-2016

Barker, S., Greaves, M., & Elderfield, H. (2003). A study of cleaning procedures used for foraminiferal Mg/Ca paleothermometry. *Geochemistry, Geophysics, Geosystems*, *4*(9), 8407. https://doi.org/10.1029/2003GC000559

Blaauw, M., & Christen, J. A. (2011). Flexible paleoclimate age-depth models using an autoregressive gamma process. *Bayesian Analysis*, *6*(3), 457–474. https://doi.org/10.1214/11-BA618

Boer, W., Nordstad, S., Weber, M., Mertz-Kraus, R., Hönisch, B., Bijma, J., et al. (2022). New calcium carbonate nano-particulate pressed powder pellet (NFHS-2-NP) for LA-ICP-OES, LA-(MC)-ICP-MS and μXRF. *Geostandards and Geoanalytical Research*, *46*(3), 411–432. https://doi.org/10.1111/ggr.12425

Boussetta, S., Bassinot, F., Sabbatini, A., Caillon, N., Nouet, J., Kallel, N., et al. (2011). Diagenetic Mg-rich calcite in Mediterranean sediments: Quantification and impact on foraminiferal Mg/Ca thermometry. *Marine Geology*, *280*(1–4), 195–204. https://doi.org/10.1016/j.margeo.2010.12.011

Branson, O., Kaczmarek, K., Redfern, S. A., Misra, S., Langer, G., Tyliszczak, T., et al. (2015). The coordination and distribution of B in foraminiferal calcite. *Earth and Planetary Science Letters*, *416*, 67–72. https://doi.org/10.1016/j.epsl.2015.02.006

Brown, R. E., Anderson, L. D., Thomas, E., & Zachos, J. C. (2011). A core-top calibration of B/Ca in the benthic foraminifers *Nuttallides umbonifera* and *Oridorsalis umbonatus*: A proxy for Cenozoic bottom water carbonate saturation. *Earth and Planetary Science Letters*, *310*(3–4), 360–368. https://doi.org/10.1016/j.epsl.2011.08.023

Brown, S. J., & Elderfield, H. (1996). Variations in Mg/Ca and Sr/Ca ratios of planktonic foraminifera caused by postdepositional dissolution: Evidence of shallow Mg-dependent dissolution. *Paleoceanography*, *11*(5), 543–551. https://doi.org/10.1029/96PA01491

Bryan, S. P., & Marchitto, T. M. (2008). Mg/Ca–temperature proxy in benthic foraminifera: New calibrations from the Florida Straits and a hypothesis regarding Mg/Li. *Paleoceanography*, *23*(2), PA2220. https://doi.org/10.1029/2007PA001553

Busenberg, E., & Plummer, L. N. (1985). Kinetic and thermodynamic factors controlling the distribution of SO_3^{2-} and Na^+ in calcites and selected aragonites. *Geochimica et Cosmochimica Acta*, *49*(3), 713–725. https://doi.org/10.1016/0016-7037(85)90166-8

Case, D. H., Robinson, L. F., Auro, M. E., & Gagnon, A. C. (2010). Environmental and biological controls on Mg and Li in deep-sea scleractinian corals. *Earth and Planetary Science Letters*, *300*(3–4), 215–225. https://doi.org/10.1016/j.epsl.2010.09.029

Cléroux, C., Cortijo, E., Anand, P., Labeyrie, L., Bassinot, F., Caillon, N., & Duplessy, J. C. (2008). Mg/Ca and Sr/Ca ratios in planktonic foraminifera: Proxies for upper water column temperature reconstruction. *Paleoceanography*, *23*(3), PA3214. https://doi.org/10.1029/2007PA001505

Coadic, R., Bassinot, F., Dissard, D., Douville, E., Greaves, M., & Michel, E. (2013). A core-top study of dissolution effect on B/Ca in *Globigerinoides sacculifer* from the tropical Atlantic: Potential bias for paleo-reconstruction of seawater carbonate chemistry. *Geochemistry, Geophysics, Geosystems*, *14*(4), 1053–1068. https://doi.org/10.1029/2012GC004296

Cuny-Guirriec, K., Douville, E., Reynaud, S., Allemand, D., Bordier, L., Canesi, M., et al. (2019). Coral Li/Mg thermometry: Caveats and constraints. *Chemical Geology*, *523*, 162–178. https://doi.org/10.1016/j.chemgeo.2019.03.038

Dämmer, L. K., de Nooijer, L., van Sebille, E., Haak, J. G., & Reichart, G.-J. (2020). Evaluation of oxygen isotopes and trace elements in planktonic foraminifera from the Mediterranean Sea as recorders of seawater oxygen isotopes and salinity. *Climate of the Past*, *16*(6), 2401–2414. https://doi.org/10.5194/cp-16-2401-2020

Darling, K. F., & Wade, C. M. (2008). The genetic diversity of planktic foraminifera and the global distribution of ribosomal RNA genotypes. *Marine Micropaleontology*, *67*(3), 216–238. https://doi.org/10.1016/j.marmicro.2008.01.009

Davis, K. J., Dove, P. M., Wasylenki, L. E., & De Yoreo, J. J. (2004). Morphological consequences of differential Mg^{2+} incorporation at structurally distinct steps on calcite. *American Mineralogist*, *89*(5–6), 714–720. https://doi.org/10.2138/am-2004-5-605

Dekens, P. S., Lea, D. W., Pak, D. K., & Spero, H. J. (2002). Core top calibration of Mg/Ca in tropical foraminifera: Refining paleotemperature estimation. *Geochemistry, Geophysics, Geosystems*, *3*(4), 1–29. https://doi.org/10.1029/2001GC000200

de Villiers, S., Greaves, M., & Elderfield, H. (2002). An intensity ratio calibration method for the accurate determination of Mg/Ca and Sr/Ca of marine carbonates by ICP-AES. *Geochemistry, Geophysics, Geosystems*, *3*(1), 1001. https://doi.org/10.1029/2001GC000169

Dissard, D., Reichart, G. J., Menkes, C., Mangeas, M., Frickenhaus, S., & Bijma, J. (2021). Mg/Ca, Sr/Ca and stable isotopes from the planktonic foraminifera *T. sacculifer*: Testing a multi-proxy approach for inferring paleotemperature and paleosalinity. *Biogeosciences*, *18*(2), 423–439. https://doi.org/10.5194/bg-18-423-2021

Dueñas-Bohórquez, A., da Rocha, R. E., Kuroyanagi, A., Bijma, J., & Reichart, G.-J. (2009). Effect of salinity and seawater calcite saturation state on Mg and Sr incorporation in cultured planktonic foraminifera. *Marine Micropaleontology*, *73*(3–4), 178–189. https://doi.org/10.1016/j.marmicro.2009.09.002

Elderfield, H., Vautravers, M., & Cooper, M. (2002). The relationship between shell size and Mg/Ca, Sr/Ca, $\delta^{18}O$, and $\delta^{13}C$ of species of planktonic foraminifera. *Geochemistry, Geophysics, Geosystems*, *3*(8), 1–13. https://doi.org/10.1029/2001GC000194

Elderfield, H., Yu, J., Anand, P., Kiefer, T., & Nyland, B. (2006). Calibrations for benthic foraminiferal Mg/Ca paleothermometry and the carbonate ion hypothesis. *Earth and Planetary Science Letters*, *250*(3–4), 633–649. https://doi.org/10.1016/j.epsl.2006.07.041

Evans, D., Wade, B. S., Henehan, M., Erez, J., & Müller, W. (2016). Revisiting carbonate chemistry controls on planktic foraminifera Mg/Ca: Implications for sea surface temperature and hydrology shifts over the Paleocene–Eocene Thermal Maximum and Eocene–Oligocene transition. *Climate of the Past*, *12*(4), 819–835. https://doi.org/10.5194/cp-12-819-2016

Evans, R. C. (1966). *An introduction to crystal chemistry*. Cambridge University Press.

15252027, 2024, 4, Downloaded from https://agupubs.onlinelibrary.wiley.com/doi/10.1029/2023GC011302 by Cochrane Netherlands, Wiley Online Library on [19/04/2024]. See the Terms and Conditions (https://onlinelibrary.wiley.com/terms-and-conditions) on Wiley Online Library for rules of use; OA articles are governed by the applicable Creative Commons License

Fallon, S. J., McCulloch, M. T., & Alibert, C. (2003). Examining water temperature proxies in Porites corals from the Great Barrier reef: A cross-shelf comparison. *Coral Reefs*, *22*(4), 389–404. https://doi.org/10.1007/s00338-003-0322-5

Farmer, J. R., Branson, O., Uchikawa, J., Penman, D. E., Hönisch, B., & Zeebe, R. E. (2019). Boric acid and borate incorporation in inorganic calcite inferred from B/Ca, boron isotopes and surface kinetic modeling. *Geochimica et Cosmochimica Acta*, *244*, 229–247. https://doi.org/10.1016/j.gca.2018.10.008

Ferguson, J., Henderson, G., Kucera, M., & Rickaby, R. (2008). Systematic change of foraminiferal Mg/Ca ratios across a strong salinity gradient. *Earth and Planetary Science Letters*, *265*(1–2), 153–166. https://doi.org/10.1016/j.epsl.2007.10.011

Fernández-Díaz, L., Fernández-González, Á., & Prieto, M. (2010). The role of sulfate groups in controlling $CaCO_3$ polymorphism. *Geochimica et Cosmochimica Acta*, *74*(21), 6064–6076. https://doi.org/10.1016/j.gca.2010.08.010

Foster, G. L. (2008). Seawater pH, pCO_2 and $[CO_3^{2-}]$ variations in the Caribbean Sea over the last 130 kyr: A boron isotope and B/Ca study of planktic foraminifera. *Earth and Planetary Science Letters*, *271*(1–4), 254–266. https://doi.org/10.1016/j.epsl.2008.04.015

Foster, G. L., & Rae, J. W. (2016). Reconstructing ocean pH with boron isotopes in foraminifera. *Annual Review of Earth and Planetary Sciences*, *44*(1), 207–237. https://doi.org/10.1146/annurev-earth-060115-012226

Fowell, S. E., Sandford, K., Stewart, J. A., Castillo, K. D., Ries, J. B., & Foster, G. L. (2016). Intrareef variations in Li/Mg and Sr/Ca sea surface temperature proxies in the Caribbean reef-building coral *Siderastrea siderea*. *Paleoceanography*, *31*(10), 1315–1329. https://doi.org/10.1002/2016PA002968

Geerken, E., de Nooijer, L., Toyofuku, T., Roepert, A., Middelburg, J. J., Kienhuis, M. V., et al. (2022). High precipitation rates characterize biomineralization in the benthic foraminifer *Ammonia beccarii*. *Geochimica et Cosmochimica Acta*, *318*, 70–82. https://doi.org/10.1016/j.gca.2021.11.026

Geerken, E., de Nooijer, L. J., Roepert, A., Polerecky, L., King, H. E., & Reichart, G. J. (2019). Element banding and organic linings within chamber walls of two benthic foraminifera. *Scientific Reports*, *9*(1), 3598. https://doi.org/10.1038/s41598-019-40298-y

Goetschl, K. E., Purgstaller, B., Dietzel, M., & Mavromatis, V. (2019). Effect of sulfate on magnesium incorporation in low-magnesium calcite. *Geochimica et Cosmochimica Acta*, *265*, 505–519. https://doi.org/10.1016/j.gca.2019.07.024

Gray, W. R., & Evans, D. (2019). Nonthermal influences on Mg/Ca in planktonic foraminifera: A review of culture studies and application to the last glacial maximum. *Paleoceanography and Paleoclimatology*, *34*(3), 306–315. https://doi.org/10.1029/2018PA003517

Gray, W. R., Weldeab, S., Lea, D. W., Rosenthal, Y., Gruber, N., Donner, B., & Fischer, G. (2018). The effects of temperature, salinity, and the carbonate system on Mg/Ca in *Globigerinoides ruber* (white): A global sediment trap calibration. *Earth and Planetary Science Letters*, *482*, 607–620. https://doi.org/10.1016/j.epsl.2017.11.026

Guillong, M., Meier, D. L., Allan, M. M., Heinrich, C. A., & Yardley, B. W. (2008). Appendix A6: SILLS: A MATLAB-based program for the reduction of laser ablation ICP-MS data of homogeneous materials and inclusions. *Mineralogical Association of Canada Short Course*, *40*, 328–333.

Guo, J., Li, T., Xiong, Z., Qiu, X., & Chang, F. (2019). Revisiting the dependence of thermocline-dwelling foraminiferal B/Ca on temperature and $[CO_3^{2-}]$, and its application in reconstruction of the subsurface carbonate system in the tropical western Pacific since 24 ka. *Acta Oceanologica Sinica*, *38*(9), 71–86. https://doi.org/10.1007/s13131-019-1476-y

Harris, C. R., Millman, K. J., van der Walt, S. J., Gommers, R., Virtanen, P., Cournapeau, D., et al. (2020). Array programming with NumPy. *Nature*, *585*(7825), 357–362. https://doi.org/10.1038/s41586-020-2649-2

Hathorne, E. C., Felis, T., Suzuki, A., Kawahata, H., & Cabioch, G. (2013). Lithium in the aragonite skeletons of massive *Porites* corals: A new tool to reconstruct tropical sea surface temperatures. *Paleoceanography*, *28*(1), 143–152. https://doi.org/10.1029/2012PA002311

Haynes, L. L., Hönisch, B., Dyez, K. A., Holland, K., Rosenthal, Y., Fish, C. R., et al. (2017). Calibration of the B/Ca proxy in the planktic foraminifer *Orbulina universa* to Paleocene seawater conditions. *Paleoceanography*, *32*(6), 580–599. https://doi.org/10.1002/2016PA003069

Haynes, L. L., Hönisch, B., Holland, K., Rosenthal, Y., & Eggins, S. M. (2019). Evaluating the planktic foraminiferal B/Ca proxy for application to deep time paleoceanography. *Earth and Planetary Science Letters*, *528*, 115824. https://doi.org/10.1016/j.epsl.2019.115824

Hemming, N., & Hanson, G. (1992). Boron isotopic composition and concentration in modern marine carbonates. *Geochimica et Cosmochimica Acta*, *56*(1), 537–543. https://doi.org/10.1016/0016-7037(92)90151-8

Hemming, N. G., Reeder, R. J., & Hart, S. R. (1998). Growth-step-selective incorporation of boron on the calcite surface. *Geochimica et Cosmochimica Acta*, *62*(17), 2915–2922. https://doi.org/10.1016/S0016-7037(98)00214-2

Henehan, M. J., Foster, G. L., Rae, J. W., Prentice, K. C., Erez, J., Bostock, H. C., et al. (2015). Evaluating the utility of B/C a ratios in planktic foraminifera as a proxy for the carbonate system: A case study of *Globigerinoides ruber*. *Geochemistry, Geophysics, Geosystems*, *16*(4), 1052–1069. https://doi.org/10.1002/2014GC005514

Hönisch, B., & Hemming, N. G. (2005). Surface ocean pH response to variations in pCO_2 through two full glacial cycles. *Earth and Planetary Science Letters*, *236*(1), 305–314. https://doi.org/10.1016/j.epsl.2005.04.027

Hover, V. C., Walter, L. M., & Peacor, D. R. (2001). Early marine diagenesis of biogenic aragonite and Mg-calcite: New constraints from high-resolution STEM and AEM analyses of modern platform carbonates. *Chemical Geology*, *175*(3–4), 221–248. https://doi.org/10.1016/S0009-2541(00)00326-0

Karancz, S., de Nooijer, L. J., Brummer, G.-J. A., Lattaud, J., Haghipour, N., Rosenthal, Y., & Reichart, G.-J. (2024). Dataset belonging to "impact of seawater inorganic carbon chemistry on element incorporation in foraminiferal shell carbonate". Version V1 [Dataset]. *NIOZ*. https://doi.org/10.25850/nioz/7b.b.5g

Keul, N., Langer, G., de Nooijer, L. J., Nehrke, G., Reichart, G. J., & Bijma, J. (2013). Incorporation of uranium in benthic foraminiferal calcite reflects seawater carbonate ion concentration. *Geochemistry, Geophysics, Geosystems*, *14*(1), 102–111. https://doi.org/10.1029/2012GC004330

Keul, N., Langer, G., Thoms, S., de Nooijer, L. J., Reichart, G.-J., & Bijma, J. (2017). Exploring foraminiferal Sr/Ca as a new carbonate system proxy. *Geochimica et Cosmochimica Acta*, *202*, 374–386. https://doi.org/10.1016/j.gca.2016.11.022

Khider, D., Huerta, G., Jackson, C., Stott, L., & Emile-Geay, J. (2015). A Bayesian, multivariate calibration for *Globigerinoides ruber* Mg/Ca. *Geochemistry, Geophysics, Geosystems*, *16*(9), 2916–2932. https://doi.org/10.1002/2015GC005844

Kincaid, E., Thunell, R. C., Le, J., Lange, C. B., Weinheimer, A. L., & Reid, F. M. H. (2000). Planktonic foraminiferal fluxes in the Santa Barbara basin: Response to seasonal and interannual hydrographic changes. *Deep Sea Research Part II: Topical Studies in Oceanography*, *47*(5), 1157–1176. https://doi.org/10.1016/S0967-0645(99)00140-X

Kısakürek, B., Eisenhauer, A., Böhm, F., Garbe-Schönberg, D., & Erez, J. (2008). Controls on shell Mg/Ca and Sr/Ca in cultured planktonic foraminiferan, *Globigerinoides ruber* (white). *Earth and Planetary Science Letters*, *273*(3–4), 260–269. https://doi.org/10.1016/j.epsl.2008.06.026

Kitano, Y., Okumura, M., & Idogaki, M. (1975). Incorporation of sodium, chloride and sulfate with calcium carbonate. *Geochemical Journal*, *9*(2), 75–84. https://doi.org/10.2343/geochemj.9.75

15252027, 2024, 4, Downloaded from https://agupubs.onlinelibrary.wiley.com/doi/10.1029/2023GC011302 by Cochrane Netherlands, Wiley Online Library on [19/04/2024]. See the Terms and Conditions (https://onlinelibrary.wiley.com/terms-and-conditions) on Wiley Online Library for rules of use; OA articles are governed by the applicable Creative Commons License

Klochko, K., Cody, G. D., Tossell, J. A., Dera, P., & Kaufman, A. J. (2009). Re-evaluating boron speciation in biogenic calcite and aragonite using ^{11}B MAS NMR. *Geochimica et Cosmochimica Acta*, *73*(7), 1890–1900. https://doi.org/10.1016/j.gca.2009.01.002

Kontrec, J., Kralj, D., Brečević, L., Falini, G., Fermani, S., Noethig-Laslo, V., & Mirosavljević, K. (2004). Incorporation of inorganic anions in calcite. *European Journal of Inorganic Chemistry*, *2004*(23), 4579–4585. https://doi.org/10.1002/ejic.200400268

Kozdon, R., Kelly, D. C., Kitajima, K., Strickland, A., Fournelle, J. H., & Valley, J. W. (2013). In situ δ^{18}O and Mg/Ca analyses of diagenetic and planktic foraminiferal calcite preserved in a deep-sea record of the Paleocene-Eocene thermal maximum. *Paleoceanography*, *28*(3), 517–528. https://doi.org/10.1002/palo.20048

Krupinski, N. B. Q., Russell, A. D., Pak, D. K., & Paytan, A. (2017). Core-top calibration of B/Ca in Pacific Ocean *Neogloboquadrina incompta* and *Globigerina bulloides* as a surface water carbonate system proxy. *Earth and Planetary Science Letters*, *466*, 139–151. https://doi.org/10.1016/j.epsl.2017.03.007

Kunioka, D., Shirai, K., Takahata, N., Sano, Y., Toyofuku, T., & Ujiie, Y. (2006). Microdistribution of Mg/Ca, Sr/Ca, and Ba/Ca ratios in *Pulleniatina obliquiloculata* test by using a NanoSIMS: Implication for the vital effect mechanism. *Geochemistry, Geophysics, Geosystems*, *7*(12), Q12P20. https://doi.org/10.1029/2006GC001280

Lauvset, S. K., Lange, N., Tanhua, T., Bittig, H. C., Olsen, A., Kozyr, A., et al. (2022). GLODAPv2. 2022: The latest version of the global interior ocean biogeochemical data product. *Earth System Science Data*, *14*(12), 5543–5572. https://doi.org/10.5194/essd-14-5543-2022

Lea, D. W., Mashiotta, T. A., & Spero, H. J. (1999). Controls on magnesium and strontium uptake in planktonic foraminifera determined by live culturing. *Geochimica et Cosmochimica Acta*, *63*(16), 2369–2379. https://doi.org/10.1016/S0016-7037(99)00197-0

Marchitto, T. M. (2006). Precise multielemental ratios in small foraminiferal samples determined by sector field ICP-MS. *Geochemistry, Geophysics, Geosystems*, *7*(5), Q05P13. https://doi.org/10.1029/2005GC001018

Mashiotta, T. A., Lea, D. W., & Spero, H. J. (1999). Glacial–interglacial changes in Subantarctic sea surface temperature and δ^{18}O-water using foraminiferal Mg. *Earth and Planetary Science Letters*, *170*(4), 417–432. https://doi.org/10.1016/S0012-821X(99)00116-8

Maslen, E., Streltsov, V., Streltsova, N., & Ishizawa, N. (1995). Electron density and optical anisotropy in rhombohedral carbonates. III. Synchrotron X-ray studies of $CaCO_3$, $MgCO_3$ and $MnCO_3$. *Acta Crystallographica Section B Structural Science*, *51*(6), 929–939. https://doi.org/10.1107/S0108768195006434

Mathien-Blard, E., & Bassinot, F. (2009). Salinity bias on the foraminifera Mg/Ca thermometry: Correction procedure and implications for past ocean hydrographic reconstructions. *Geochemistry, Geophysics, Geosystems*, *10*(12), Q12011. https://doi.org/10.1029/2008GC002353

Mewes, A., Langer, G., Reichart, G.-J., de Nooijer, L. J., Nehrke, G., & Bijma, J. (2015). The impact of Mg contents on Sr partitioning in benthic foraminifers. *Chemical Geology*, *412*, 92–98. https://doi.org/10.1016/j.chemgeo.2015.06.026

Mezger, E., De Nooijer, L., Boer, W., Brummer, G., & Reichart, G. (2016). Salinity controls on Na incorporation in Red Sea planktonic foraminifera. *Paleoceanography*, *31*(12), 1562–1582. https://doi.org/10.1002/2016PA003052

Midgley, S. D., Di Tommaso, D., Fleitmann, D., & Grau-Crespo, R. (2021). Sulfate and molybdate incorporation at the calcite–water interface: Insights from ab initio molecular dynamics. *ACS Earth and Space Chemistry*, *5*(8), 2066–2073. https://doi.org/10.1021/acsearthspacechem.1c00131

Montagna, P., McCulloch, M., Douville, E., Correa, M. L., Trotter, J., Rodolfo-Metalpa, R., et al. (2014). Li/Mg systematics in scleractinian corals: Calibration of the thermometer. *Geochimica et Cosmochimica Acta*, *132*, 288–310. https://doi.org/10.1016/j.gca.2014.02.005

Müller, T., Karancz, S., Mattioli, E., Milovský, R., Pálfy, J., Schlögl, J., et al. (2020). Assessing anoxia, recovery and carbonate production setback in a hemipelagic Tethyan basin during the Toarcian oceanic anoxic event (Western Carpathians). *Global and Planetary Change*, *195*, 103366. https://doi.org/10.1016/j.gloplacha.2020.103366

Ni, S., Quintana Krupinski, N. B., Groeneveld, J., Persson, P., Somogyi, A., Brinkmann, I., et al. (2020). Early diagenesis of foraminiferal calcite under anoxic conditions: A case study from the Landsort Deep, Baltic Sea (IODP site M0063). *Chemical Geology*, *558*, 119871. https://doi.org/10.1016/j.chemgeo.2020.119871

Ni, Y., Foster, G. L., Bailey, T., Elliott, T., Schmidt, D. N., Pearson, P., et al. (2007). A core top assessment of proxies for the ocean carbonate system in surface-dwelling foraminifers. *Paleoceanography*, *22*(3), PA3212. https://doi.org/10.1029/2006PA001337

Nielsen, L. C., De Yoreo, J. J., & DePaolo, D. J. (2013). General model for calcite growth kinetics in the presence of impurity ions. *Geochimica et Cosmochimica Acta*, *115*, 100–114. https://doi.org/10.1016/j.gca.2013.04.001

Nürnberg, D., Bijma, J., & Hemleben, C. (1996). Assessing the reliability of magnesium in foraminiferal calcite as a proxy for water mass temperatures. *Geochimica et Cosmochimica Acta*, *60*(5), 803–814. https://doi.org/10.1016/0016-7037(95)00446-7

Okumura, M., & Kitano, Y. (1986). Coprecipitation of alkali metal ions with calcium carbonate. *Geochimica et Cosmochimica Acta*, *50*(1), 49–58. https://doi.org/10.1016/0016-7037(86)90047-5

Okumura, T., Kim, H.-J., Kim, J.-W., & Kogure, T. (2018). Sulfate-containing calcite: Crystallographic characterization of natural and synthetic materials. *European Journal of Mineralogy*, *30*(5), 929–937. https://doi.org/10.1127/ejm/2018/0030-2772

Osborne, E. B., Umling, N. E., Bizimis, M., Buckley, W., Sadekov, A., Tappa, E., et al. (2020). A sediment trap evaluation of B/Ca as a carbonate system proxy in asymbiotic and nondinoflagellate hosting planktonic foraminifera. *Paleoceanography and Paleoclimatology*, *35*(2), e2019PA003682. https://doi.org/10.1029/2019PA003682

Pagani, M. (2014). Biomarker-based inferences of past climate: The alkenone pCO_2 proxy. In *Treatise on Geochemistry* (pp. 361–378). https://doi.org/10.1016/b978-0-08-095975-7.01027-5

Pagani, M., Freeman, K. H., Ohkouchi, N., & Caldeira, K. (2002). Comparison of water column [CO_{2aq}] with sedimentary alkenone-based estimates: A test of the alkenone-CO_2 proxy. *Paleoceanography*, *17*(4). https://doi.org/10.1029/2002pa000756

Pagani, M., Zachos, J. C., Freeman, K. H., Tipple, B., & Bohaty, S. (2005). Marked decline in atmospheric carbon dioxide concentrations during the Paleogene. *Science*, *309*(5734), 600–603. https://doi.org/10.1126/science.1110063

Panieri, G., Lepland, A., Whitehouse, M. J., Wirth, R., Raanes, M. P., James, R. H., et al. (2017). Diagenetic Mg-calcite overgrowths on foraminiferal tests in the vicinity of methane seeps. *Earth and Planetary Science Letters*, *458*, 203–212. https://doi.org/10.1016/j.epsl.2016.10.024

Paquette, J., & Reeder, R. J. (1990). New type of compositional zoning in calcite: Insights into crystal-growth mechanisms. *Geology*, *18*(12), 1244. https://doi.org/10.1130/0091-7613(1990)018

Paquette, J., Vali, H., & Mucci, A. (1996). TEM study of Pt-C replicas of calcite overgrowths precipitated from electrolyte solutions. *Geochimica et Cosmochimica Acta*, *60*(23), 4689–4699. https://doi.org/10.1016/S0016-7037(96)00270-0

Pedregosa, F., Varoquaux, G., Gramfort, A., Michel, V., Thirion, B., Grisel, O., et al. (2011). Scikit-learn: Machine learning in Python. *Journal of Machine Learning Research*, *12*, 2825–2830.

Pingitore, N. E., Meitzner, G., & Love, K. M. (1995). Identification of sulfate in natural carbonates by X-ray absorption spectroscopy. *Geochimica et Cosmochimica Acta*, *59*(12), 2477–2483. https://doi.org/10.1016/0016-7037(95)00142-5

Pingitore, N. E., Meitzner, G., & Love, K. M. (1997). Discrimination of sulfate from sulfide in carbonates by electron probe microanalysis. *Carbonates and Evaporites*, *12*(1), 130–133. https://doi.org/10.1007/BF03175812

15252027, 2024, 4, Downloaded from https://agupubs.onlinelibrary.wiley.com/doi/10.1029/2023GC011302 by Cochrane Netherlands, Wiley Online Library on [19/04/2024]. See the Terms and Conditions (https://onlinelibrary.wiley.com/terms-and-conditions) on Wiley Online Library for rules of use; OA articles are governed by the applicable Creative Commons License

Pokroy, B., Fitch, A. N., Marin, F., Kapon, M., Adir, N., & Zolotoyabko, E. (2006). Anisotropic lattice distortions in biogenic calcite induced by intra-crystalline organic molecules. *Journal of Structural Biology*, *155*(1), 96–103. https://doi.org/10.1016/j.jsb.2006.03.008

Raddatz, J., Liebetrau, V., Rüggeberg, A., Hathorne, E., Krabbenhöft, A., Eisenhauer, A., et al. (2013). Stable Sr-isotope, Sr/Ca, Mg/Ca, Li/Ca, and Mg/Li ratios in the scleractinian cold-water coral *Lophelia pertusa*. *Chemical Geology*, *352*, 143–152. https://doi.org/10.1016/j.chemgeo.2013.06.013

Rae, J. W. B., Foster, G. L., Schmidt, D. N., & Elliott, T. (2011). Boron isotopes and B/Ca in benthic foraminifera: Proxies for the deep ocean carbonate system. *Earth and Planetary Science Letters*, *302*(3–4), 403–413. https://doi.org/10.1016/j.epsl.2010.12.034

Raitzsch, M., Bijma, J., Benthien, A., Richter, K.-U., Steinhoefel, G., & Kučera, M. (2018). Boron isotope-based seasonal paleo-pH reconstruction for the Southeast Atlantic—A multispecies approach using habitat preference of planktonic foraminifera. *Earth and Planetary Science Letters*, *487*, 138–150. https://doi.org/10.1016/j.epsl.2018.02.002

Raitzsch, M., Kuhnert, H., Hathorne, E. C., Groeneveld, J., & Bickert, T. (2011). U/Ca in benthic foraminifers: A proxy for the deep-sea carbonate saturation. *Geochemistry, Geophysics, Geosystems*, *12*(6), Q06019. https://doi.org/10.1029/2010GC003344

Regenberg, M., Nürnberg, D., Schönfeld, J., & Reichart, G.-J. (2007). Early diagenetic overprint in Caribbean sediment cores and its effect on the geochemical composition of planktonic foraminifera. *Biogeosciences*, *4*(6), 957–973. https://doi.org/10.5194/bg-4-957-2007

Reichart, G.-J., Jorissen, F., Anschutz, P., & Mason, P. R. (2003). Single foraminiferal test chemistry records the marine environment. *Geology*, *31*(4), 355–358. https://doi.org/10.1130/0091-7613(2003)031

Rosenthal, Y., Bova, S., & Zhou, X. (2022). A user guide for choosing planktic foraminiferal Mg/Ca-temperature calibrations. *Paleoceanography and Paleoclimatology*, *37*(6), e2022PA004413. https://doi.org/10.1029/2022PA004413

Rosenthal, Y., Boyle, E. A., & Slowey, N. (1997). Temperature control on the incorporation of magnesium, strontium, fluorine, and cadmium into benthic foraminiferal shells from Little Bahama Bank: Prospects for thermocline paleoceanography. *Geochimica et Cosmochimica Acta*, *61*(17), 3633–3643. https://doi.org/10.1016/S0016-7037(97)00181-6

Rosenthal, Y., Lear, C. H., Oppo, D. W., & Linsley, B. K. (2006). Temperature and carbonate ion effects on Mg/Ca and Sr/Ca ratios in benthic foraminifera: Aragonitic species *Hoeglundina elegans*. *Paleoceanography*, *21*(1), PA1007. https://doi.org/10.1029/2005PA001158

Rubin, D. B. (1981). The Bayesian bootstrap. *Annals of Statistics*, *9*(1), 130–134. https://doi.org/10.1214/aos/1176345338

Ruiz-Agudo, E., Putnis, C., Kowacz, M., Ortega-Huertas, M., & Putnis, A. (2012). Boron incorporation into calcite during growth: Implications for the use of boron in carbonates as a pH proxy. *Earth and Planetary Science Letters*, *345*, 9–17. https://doi.org/10.1016/j.epsl.2012.06.032

Russell, A. D., Hönisch, B., Spero, H. J., & Lea, D. W. (2004). Effects of seawater carbonate ion concentration and temperature on shell U, Mg, and Sr in cultured planktonic foraminifera. *Geochimica et Cosmochimica Acta*, *68*(21), 4347–4361. https://doi.org/10.1016/j.gca.2004.03.013

Rutherford, S., D'Hondt, S., & Prell, W. (1999). Environmental controls on the geographic distribution of zooplankton diversity. *Nature*, *400*(6746), 749–753. https://doi.org/10.1038/23449

Sadekov, A. Y., Darling, K. F., Ishimura, T., Wade, C. M., Kimoto, K., Singh, A. D., et al. (2016). Geochemical imprints of genotypic variants of *Globigerina bulloides* in the Arabian Sea. *Paleoceanography*, *31*(10), 1440–1452. https://doi.org/10.1002/2016pa002947

Saenger, C. P., & Evans, M. N. (2019). Calibration and validation of environmental controls on planktic foraminifera Mg/Ca using global core-top data. *Paleoceanography and Paleoclimatology*, *34*(8), 1249–1270. https://doi.org/10.1029/2018PA003507

Schenau, S., Passier, H., Reichart, G.-J., & De Lange, G. (2002). Sedimentary pyrite formation in the Arabian Sea. *Marine Geology*, *185*(3–4), 393–402. https://doi.org/10.1016/S0025-3227(02)00183-4

Schlitzer, R. (2022). Ocean data view. Retrieved from https://odv.awi.de/

Sen, S., Stebbins, J., Hemming, N., & Ghosh, B. (1994). Coordination environments of B impurities in calcite and aragonite polymorphs: A ^{11}B MAS NMR study. *American Mineralogist*, *79*(9–10), 819–825.

Sexton, P. F., Wilson, P. A., & Pearson, P. N. (2006). Microstructural and geochemical perspectives on planktic foraminiferal preservation: "Glassy" versus "Frosty". *Geochemistry, Geophysics, Geosystems*, *7*(12), Q12P19. https://doi.org/10.1029/2006gc001291

Stainbank, S., Spezzaferri, S., De Boever, E., Bouvier, A.-S., Chilcott, C., De Leau, E. S., et al. (2020). Assessing the impact of diagenesis on foraminiferal geochemistry from a low latitude, shallow-water drift deposit. *Earth and Planetary Science Letters*, *545*, 116390. https://doi.org/10.1016/j.epsl.2020.116390

Staudt, W. J., Reeder, R. J., & Schoonen, M. A. (1994). Surface structural controls on compositional zoning of SO_4^{2-} and SeO_4^{2-} in synthetic calcite single crystals. *Geochimica et Cosmochimica Acta*, *58*(9), 2087–2098. https://doi.org/10.1016/0016-7037(94)90287-9

Steinke, S., Chiu, H.-Y., Yu, P.-S., Shen, C.-C., Löwemark, L., Mii, H.-S., & Chen, M.-T. (2005). Mg/Ca ratios of two *Globigerinoides ruber* (white) morphotypes: Implications for reconstructing past tropical/subtropical surface water conditions. *Geochemistry, Geophysics, Geosystems*, *6*(11), Q11005. https://doi.org/10.1029/2005gc000926

Takano, B. (1985). Geochemical implications of sulfate in sedimentary carbonates. *Chemical Geology*, *49*(4), 393–403. https://doi.org/10.1016/0009-2541(85)90001-4

Tripati, A. K., Roberts, C. D., & Eagle, R. A. (2009). Coupling of CO_2 and ice sheet stability over major climate transitions of the last 20 million years. *Science*, *326*(5958), 1394–1397. https://doi.org/10.1126/science.1178296

Uchikawa, J., Harper, D. T., Penman, D. E., Zachos, J. C., & Zeebe, R. E. (2017). Influence of solution chemistry on the boron content in inorganic calcite grown in artificial seawater. *Geochimica et Cosmochimica Acta*, *218*, 291–307. https://doi.org/10.1016/j.gca.2017.09.016

Uchikawa, J., Penman, D. E., Harper, D. T., Farmer, J. R., Zachos, J. C., Planavsky, N. J., & Zeebe, R. E. (2023). Sulfate and phosphate oxyanions alter B/Ca and δ^{11}B in inorganic calcite at constant pH: Crystallographic controls outweigh normal kinetic effects. *Geochimica et Cosmochimica Acta*, *343*, 353–370. https://doi.org/10.1016/j.gca.2022.12.018

Uchikawa, J., Penman, D. E., Zachos, J. C., & Zeebe, R. E. (2015). Experimental evidence for kinetic effects on B/Ca in synthetic calcite: Implications for potential $B(OH)_4^-$ and $B(OH)_3$ incorporation. *Geochimica et Cosmochimica Acta*, *150*, 171–191. https://doi.org/10.1016/j.gca.2014.11.022

Van Dijk, I., Barras, C., De Nooijer, L. J., Mouret, A., Geerken, E., Oron, S., & Reichart, G.-J. (2019). Coupled calcium and inorganic carbon uptake suggested by magnesium and sulfur incorporation in foraminiferal calcite. *Biogeosciences*, *16*(10), 2115–2130. https://doi.org/10.5194/bg-16-2115-2019

Van Dijk, I., de Nooijer, L. J., Boer, W., & Reichart, G.-J. (2017). Sulfur in foraminiferal calcite as a potential proxy for seawater carbonate ion concentration. *Earth and Planetary Science Letters*, *470*, 64–72. https://doi.org/10.1016/j.epsl.2017.04.031

Van Dijk, I., de Nooijer, L. J., Wolthers, M., & Reichart, G.-J. (2017). Impacts of pH and $[CO_3^{2-}]$ on the incorporation of Zn in foraminiferal calcite. *Geochimica et Cosmochimica Acta*, *197*, 263–277. https://doi.org/10.1016/j.gca.2016.10.031

Virtanen, P., Gommers, R., Oliphant, T. E., Haberland, M., Reddy, T., Cournapeau, D., et al. (2020). SciPy 1.0: Fundamental algorithms for scientific computing in Python. *Nature Methods*, *17*(3), 261–272. https://doi.org/10.1038/s41592-019-0686-2

15252027, 2024, 4, Downloaded from https://agupubs.onlinelibrary.wiley.com/doi/10.1029/2023GC011302 by Cochrane Netherlands, Wiley Online Library on [19/04/2024]. See the Terms and Conditions (https://onlinelibrary.wiley.com/terms-and-conditions) on Wiley Online Library for rules of use; OA articles are governed by the applicable Creative Commons License

Wacker, L., Fahrni, S. M., Hajdas, I., Molnar, M., Synal, H. A., Szidat, S., & Zhang, Y. L. (2013). A versatile gas interface for routine radiocarbon analysis with a gas ion source. *Nuclear Instruments and Methods in Physics Research Section B: Beam Interactions with Materials and Atoms*, *294*, 315–319. https://doi.org/10.1016/j.nimb.2012.02.009

Wacker, L., Güttler, D., Goll, J., Hurni, J. P., Synal, H. A., & Walti, N. (2014). Radiocarbon dating to a single year by means of rapid atmospheric ^{14}C changes. *Radiocarbon*, *56*(2), 573–579. https://doi.org/10.2458/56.17634

Wu, Y., Fallon, S. J., Cantin, N. E., & Lough, J. M. (2021). Assessing multiproxy approaches (Sr/Ca, U/Ca, Li/Mg, and B/Mg) to reconstruct sea surface temperature from coral skeletons throughout the Great Barrier Reef. *Science of the Total Environment*, *786*, 147393. https://doi.org/10.1016/j.scitotenv.2021.147393

Yu, J., Day, J., Greaves, M., & Elderfield, H. (2005). Determination of multiple element/calcium ratios in foraminiferal calcite by quadrupole ICP-MS. *Geochemistry, Geophysics, Geosystems*, *6*(8), Q08P01. https://doi.org/10.1029/2005GC000964

Yu, J., & Elderfield, H. (2007). Benthic foraminiferal B/Ca ratios reflect deep water carbonate saturation state. *Earth and Planetary Science Letters*, *258*(1–2), 73–86. https://doi.org/10.1016/j.epsl.2007.03.025

Yu, J., Elderfield, H., & Hönisch, B. (2007). B/Ca in planktonic foraminifera as a proxy for surface seawater pH. *Paleoceanography*, *22*(2), PA2202. https://doi.org/10.1029/2006pa001347

Zeebe, R. E., & Wolf-Gladrow, D. (2001). *CO_2 in seawater: Equilibrium, kinetics, isotopes*. Elsevier.

15252027, 2024, 4, Downloaded from https://agupubs.onlinelibrary.wiley.com/doi/10.1029/2023GC011302 by Cochrane Netherlands, Wiley Online Library on [19/04/2024]. See the Terms and Conditions (https://onlinelibrary.wiley.com/terms-and-conditions) on Wiley Online Library for rules of use; OA articles are governed by the applicable Creative Commons License